



# Radiolabeling lipoproteins to study and manage disease

Carlos Pérez-Medina<sup>1</sup> · Edward A. Fisher<sup>2</sup> · Zahi A. Fayad<sup>3</sup> · Willem J. M. Mulder<sup>4,5</sup> · Abraham J. P. Teunissen<sup>3,6,7</sup> 

Received: 22 January 2025 / Accepted: 9 April 2025 / Published online: 28 April 2025

© The Author(s), under exclusive licence to Springer-Verlag GmbH Germany, part of Springer Nature 2025

## Abstract

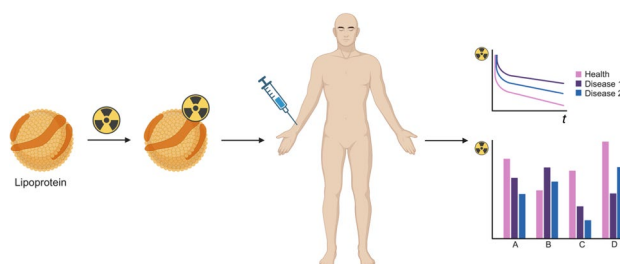
**Purpose** Lipoproteins are endogenous nanoparticles with essential roles in lipid transport and inflammation. Lipoproteins are also valuable in diagnosing and treating disease. For instance, certain lipoproteins are overexpressed in patients with atherosclerotic cardiovascular disease, and reconstituted lipoproteins have been extensively used for drug delivery. Radiolabeling has proven an especially powerful approach for studying and therapeutically exploiting lipoproteins. This review details how radiochemistry and nuclear imaging can facilitate the study of lipoproteins in health and disease. Among other topics, we discuss approaches for radiolabeling lipoproteins and detail how these have helped advance our understanding of lipoprotein biology and the diagnosis and treatment of diseases, including atherosclerosis, cancer, and hypercholesterolemia.

**Methods** We performed an extensive literature search on all peer-reviewed studies involving radiolabeled lipoproteins and selected representative examples to provide a high-level overview of the most important discoveries and technological advancements.

**Results** More than 200 peer-reviewed papers involved radiolabeled lipoproteins, spanning mechanistic, diagnostic, and therapeutic studies across a wide range of diseases.

**Conclusion** Radiolabeling has been critical in advancing our understanding of lipoprotein biology and leveraging these nanomaterials for diagnosing and treating disease.

## Graphical Abstract



**Keywords** Lipoproteins · Radiolabeling · Apolipoprotein · Positron emission tomography

✉ Willem J. M. Mulder  
willem.mulder@radboudumc.nl

✉ Abraham J. P. Teunissen  
bram.teunissen@mssm.edu

<sup>1</sup> Centro Nacional de Investigaciones Cardiovasculares (CNIC), Madrid, Spain

<sup>2</sup> Department of Medicine (Cardiology), New York University Grossman School of Medicine, New York, NY, USA

<sup>3</sup> Biomedical Engineering and Imaging Institute, Icahn School of Medicine at Mount Sinai, New York, NY, USA

<sup>4</sup> Department of Biomedical Engineering, Eindhoven University of Technology, Eindhoven, the Netherlands

<sup>5</sup> Department of Internal Medicine and Radboud Center for Infectious Diseases, Radboud University Medical Center, Nijmegen, the Netherlands

<sup>6</sup> Icahn School of Medicine at Mount Sinai, Cardiovascular Research Institute, New York, NY, USA

<sup>7</sup> Icahn Genomics Institute, Icahn School of Medicine at Mount Sinai, New York, NY, USA

## Introduction

Lipids perform a broad range of biological functions, including metabolism, immune regulation, and forming cell membranes [1–4]. Lipids are generally also poorly water-soluble, which complicates their transport in aqueous biological environments. A transport system has evolved that enables lipids to traffic *in vivo*, including blood, extracellular fluids, and interstitial fluid in the lymphatic system [5]. This system consists of lipid-protein nanoassemblies called lipoproteins. Concerning their supramolecular architecture, lipoproteins resemble an oil-in-water emulsion. A monolayer of amphiphilic phospholipids and apolipoproteins stabilizes a hydrophobic core of cholesteryl esters and triglycerides. Apolipoproteins integrate into the phospholipid monolayer and stabilize the nanoassembly through hydrophobic and electrostatic interactions, while also providing regulatory functions. High-density lipoprotein (HDL) and low-density lipoprotein (LDL) are the most well-known lipoproteins, generally referred to as good and bad cholesterol, respectively [6]. Besides HDL and LDL, the major lipoprotein classes include intermediate-density lipoprotein (IDL), very-low-density lipoprotein (VLDL), and chylomicrons, which are also referred to as ultra-low-density lipoproteins

(ULDL) (Fig. 1) [7]. Lipoprotein classification is based on electrophoretic mobility or density, with HDL showing the highest mobility, followed by LDL, IDL, VLDL, and chylomicrons [7].

While density is an important parameter, it does not fully capture other key lipoprotein aspects such as size, composition and apolipoprotein content. Lipoprotein sizes range from 5–12 nm for HDL, 18–25 nm for LDL, 25–35 nm for IDL, 30–80 nm for VLDL, and up to several hundreds of nanometers for chylomicrons [7]. Due to their unique physicochemical features and biological function, the proteins in lipoproteins, referred to as apoproteins or apolipoproteins, have a great importance. Apolipoproteins' amphiphilic nature gives them critical lipid binding capabilities, while certain amino acid sequences facilitate cellular interactions and regulatory functions. Although many types of apolipoproteins exist, this review will focus mostly on apolipoprotein A1 (apoA1), HDL's main protein constituent, and apolipoprotein B (apoB), LDL's major protein. LDL and in particular its oxidized form, oxLDL, is a major driver of cardiovascular disease, hence its name 'bad cholesterol' [9]. Conversely, HDL, or 'good cholesterol', owes its atheroprotective properties to its role in reverse cholesterol transport [10–13].

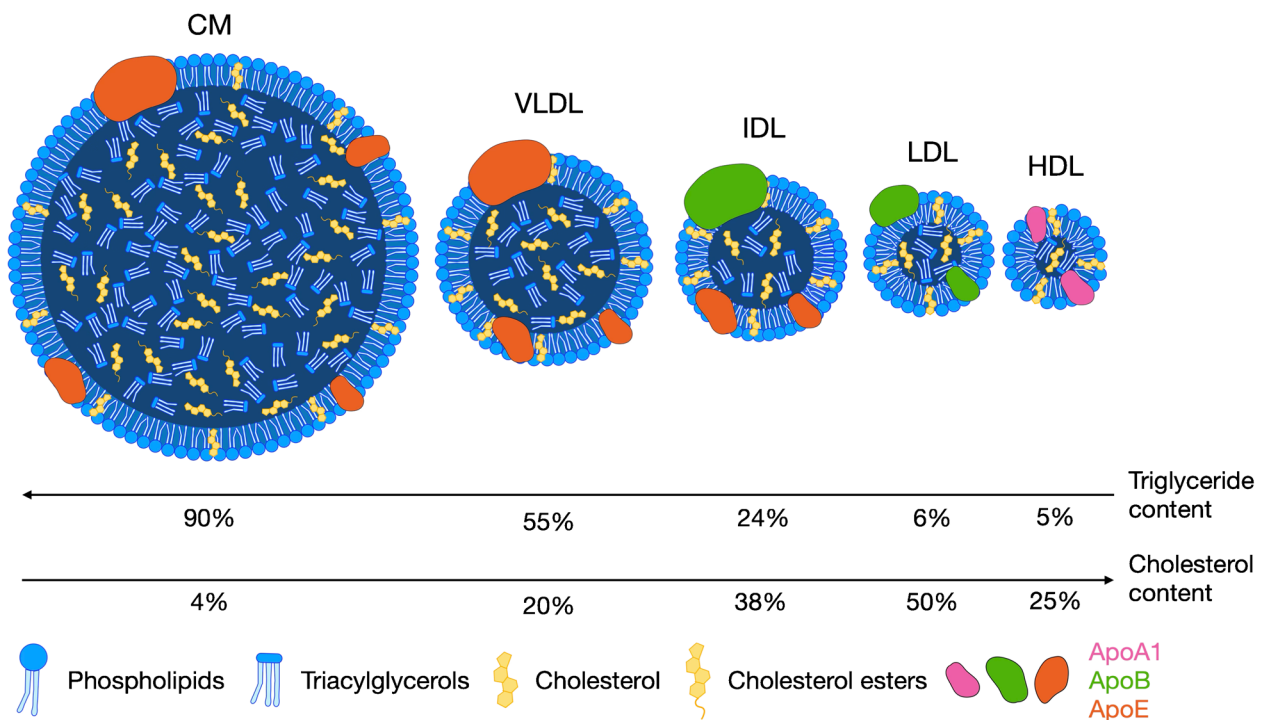


**Fig. 1** Schematic overview of the main different types of lipoproteins. Lipoproteins consist of (phospho)lipids, triacylglycerols, cholesterol (ester), and apolipoproteins. Based on their diameter and composition, lipoproteins are classified as chylomicrons (CM), very low-

density lipoprotein (VLDL), intermediate-density lipoprotein (IDL), low-density lipoprotein (LDL), and high-density lipoprotein (HDL). ApoA1 = apolipoprotein A1, apoB = apolipoprotein B, apoE = apolipoprotein E, percentages are by weight. Figure based on ref. [8]

Besides lipid transport, lipoproteins have important roles in endotoxin clearance [14, 15] and in the transport of macromolecules, including nucleic acids [16]. In 2011, Vickers, Ramaley and colleagues showed that circulating microRNAs are trafficked and delivered to cells by HDL [16]. Another interesting, but understudied feature of HDL and LDL is their transport in the lymphatics [5]. As our basic knowledge of lipoproteins' role in disease grows, opportunities for diagnostics and therapy are being evaluated. For example, HDL's atheroprotective properties have been explored for therapeutic purposes. In preclinical models, exogenously administered HDL reduces – and in some studies it reverses – atherosclerosis. Despite the overwhelming therapeutic evidence in preclinical models and in clinical observation studies, clinical trials exogenously raising HDL have not shown benefits in cardiovascular patients, with some interpreting this as a reflection of overall HDL functionality not being correlated with HDL levels [17]. Although lipoproteins and their metabolism are primarily associated with cardiovascular disease, their role in cancer makes them attractive as diagnostics or therapeutics in this condition [18].

Besides studying lipoprotein biology and physical chemistry, bioengineered versions of these nanoparticles have been studied for molecular imaging and targeted therapy. For the latter objective, lipoprotein-derived nanoparticles have been developed for siRNA delivery [19], for cancer therapy [20], and immunotherapy [21–23]. As lipoproteins display natural tropism for immune cells, the latter treatment modality holds particular promise. In the context of molecular imaging [24], HDL and LDL have been labeled with fluorophores for optical imaging [25], loaded with a superparamagnetic iron oxide core [26, 27] or Gd-DTPA-based lipids in the phospholipid corona [28–31] for magnetic resonance imaging, or packed with gold nanocrystals to allow detection by computed tomography [32].

As it is being used to study lipoprotein biology, but also for in vivo imaging and therapy, radiolabeling of lipoproteins takes a special position. The first lipoprotein radiolabeling methods were developed in the 1970's and these helped gather insights into lipoprotein pharmacokinetics and biodistribution [33–38], metabolism [39–45], and receptor distribution and function [46–48]. In later work, radiolabeling was used to study lipoprotein dysregulation in pathology [49–52], with a particular focus on atherosclerotic disease [53–57]. Besides cardiovascular disease, investigators used radiolabeled lipoproteins for the diagnosis of hypercholesterolemia [50, 58–60], cancer [61, 62], liver disease [63], obesity [64], and myeloproliferative disease [65].

This review discusses how radiolabeling lipoproteins has matured from a basic research tool and method to study lipoprotein biology to a versatile technique for in vivo nuclear imaging in preclinical models [23, 66–69] and human subjects [70]. It also highlights the latest advances in integrating

radiolabeling and in vivo imaging to develop lipoprotein-inspired, bioengineered immunotherapies. Finally, an outlook of future developments is provided.

## Radiolabeling lipoproteins

Over five decades, various lipoprotein radiolabeling methods have been developed. This section discusses existing and up-and-coming radiochemical strategies, organized by radionuclide. The following account is not intended to be exhaustive but rather to equip newcomers in the field with an understanding of the most widely used lipoprotein radiolabeling approaches.

### Radioiodine

Iodine is widely used for lipoprotein radiolabeling as the associated chemistry is well-established, iodine isotopes cover a broad range of physical half-lives, and iodine radionuclides suitable for PET and SPECT imaging are available. The most commonly used iodine radioisotopes used for labeling lipoproteins are  $^{123}\text{I}$  ( $t_{1/2} = 13.2$  h),  $^{124}\text{I}$  ( $t_{1/2} = 4.2$  d),  $^{125}\text{I}$  ( $t_{1/2} = 59.4$  d), and  $^{131}\text{I}$  ( $t_{1/2} = 8.0$  d). The iodine monochloride method developed by McFarlane [71] enables directly labeling tyrosine residues in the protein components of HDL [72–74] and LDL [75–77] by electrophilic substitution (Fig. 2A). Bilheimer et al. [78] introduced a variation to this method by involving slight changes in pH and iodine-to-protein ratio, which has been similarly used to radiolabel HDL [79, 80], LDL [54, 81–84], and VLDL [78, 85]. Different oxidants have also been used, including chloramine T [86–89], lactoperoxidase [88, 90], and solid phase oxidizing agents including 1,3,4,6-tetrachloro-3 $\alpha$ ,6 $\alpha$ -diphenyl glycoluril [82, 87, 91–93] (a.k.a. Iodogen [94]) and *N*-chloro-benzenesulfonamide-containing IODO beads [83, 95]. Although these methods predominantly functionalize apolipoproteins' tyrosine residues, some lipid radiolabeling typically occurs [87, 88]. Radioiodinated tyrosine is also prone to deiodination, resulting in free iodide that accumulates in the thyroid gland [76]. Moreover, the required oxidizing agents can extensively modify lipoproteins, altering their structure and behavior and complicating the characterization of the radioactive product [87, 91].

Lipoprotein radioiodination methods that do not require aggressive tyrosine oxidation have also been developed. In one approach, a lysine-reactive tyramine-cellobiose adduct is radiolabeled before lipoprotein conjugation using cyanuric chloride [96]. This method has been extensively used to radioiodinate LDL [75, 76, 97] and HDL [98, 99], and yields a more residualizing signal (*i.e.*, the radionuclide remains in a biological compartment longer) compared with iodine monochloride labeling. A similar method involves oxidizing

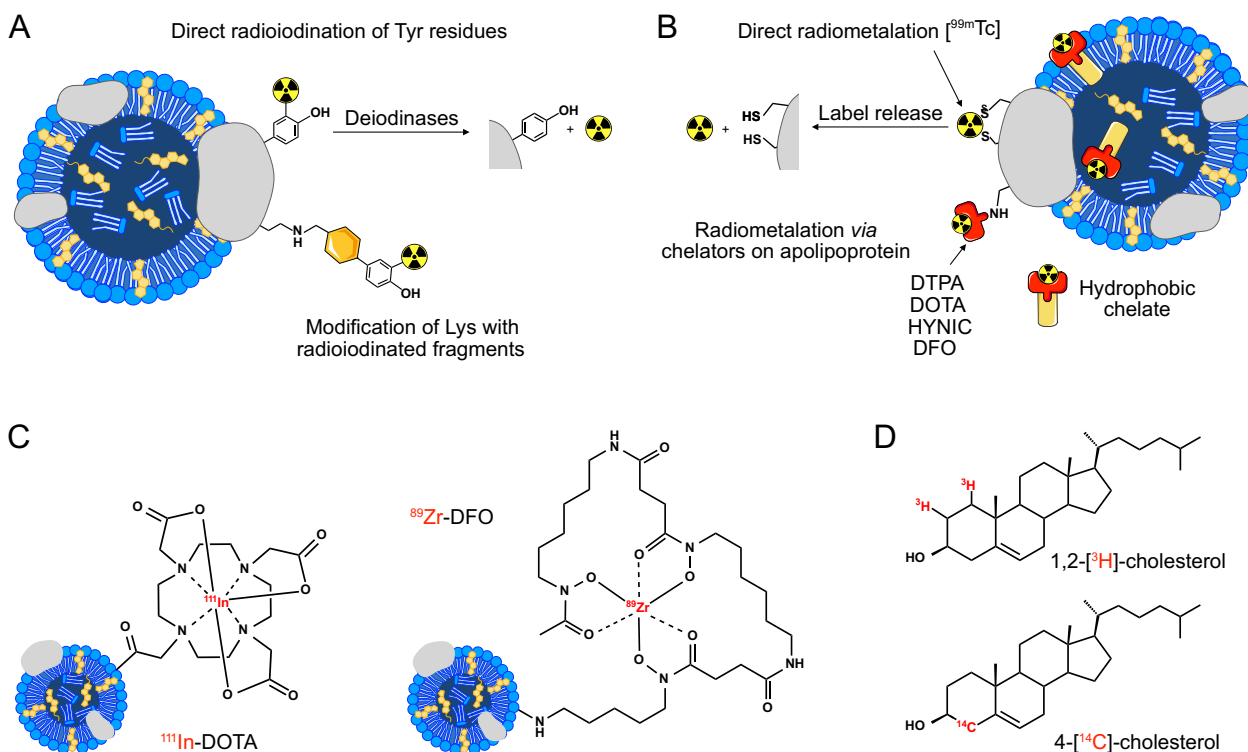


**Fig. 2** **A**) Schematic depicting the approaches for radioiodinating lipoproteins and their deiodination by enzymes. Grey structures represent apolipoproteins. **B**) Schematic depicting approaches for labeling lipoproteins with radiometals, using  $^{99m}\text{Tc}$  as an example. **C**) Structures of a lipoprotein functionalized with the chelator DOTA binding the radiometal  $^{111}\text{In}$  (left) and a lipoprotein similarly func-

tionized with deferoxamine binding  $^{89}\text{Zr}$  (right). **D**) Molecular structures of radioactive  $1,2$ -[ $^3\text{H}$ ]-cholesterol and  $4$ -[ $^{14}\text{C}$ ]-cholesterol. Parts of this figure were created using Servier Medical Art, licensed under a Creative Commons Attribution 3.0 Unported License (<https://creativecommons.org/licenses/by/3.0/>)

radioiodinated tyramine-dilactitol with galactose oxidase. The resulting aldehyde is then reacted with lipoproteins and reduced with sodium cyanoborohydride [100, 101]. Finally, the Bolton-Hunter method [102] uses a radioiodinated 3-(4-hydroxy-3-iodophenyl)propionic acid *N*-hydroxysuccinimide ester to functionalize reactive amino groups in proteins. This strategy has been used to efficiently radioiodinate the proteins in LDL [88, 97], but it also results in extensive labeling of the lipid fraction [88]. Overall, well-established approaches for labeling lipoproteins with radioactive iodine exist, and the various commercially available iodine radioisotopes enable optimizing their physical half-lives for the intended application. Moreover, the covalent nature of lipoprotein-iodine bonds limits unwanted radionuclide release. Still, most lipoprotein radioiodination procedures are relatively challenging and prone to producing side and degradation products, offering poor reproducibility and little control over which lipoprotein components are radiolabeled.

## Radiometals

The relatively mild and straightforward procedures required for non-covalently labeling lipoprotein with radiometals

make this one of the most widely used approaches. The wide availability and low cost of technetium-99m ( $^{99m}\text{Tc}$ ,  $t_{1/2} = 6.0$  h) have made it the radiometal of choice (Fig. 2B). Radiolabeling with  $^{99m}\text{Tc}$  typically involves reducing pertechnetate to generate reactive  $^{99m}\text{Tc}$  cations for non-covalent binding to a target molecule. LDL is widely labeled with  $^{99m}\text{Tc}$  using the reducing agent dithionite, enabling the chelation of  $^{99m}\text{Tc}$  by apolipoproteins' cysteine residues [53, 61, 75, 82, 103, 104]. This approach produces high urine radioactivity, presumably due to the relatively weak cysteine- $^{99m}\text{Tc}$  bond [103]. In analogous fashion, other reducing agents can also aid the labeling of LDL with  $^{99m}\text{Tc}$ , including ascorbic acid [105] and sodium borohydride with stannous chloride [53, 82, 105]. As with direct radioiodination, the reducing agents required for binding  $^{99m}\text{Tc}$  can extensively alter lipoprotein structure and behavior [105]. In a milder approach, the hydrophobic chelates  $^{99m}\text{Tc}$ -hydrazinonicotinic acid (HYNIC)-*N*-dodecylamide and  $^{99m}\text{Tc}$ -HYNIC-cholesterol are used to radiolabel reconstituted HDL (rHDL) nanoparticles [106, 107].

The radiometal indium-111 ( $^{111}\text{In}$ ) is a commonly used alternative to  $^{99m}\text{Tc}$ , as its longer physical half-life ( $t_{1/2} = 2.8$  d) enables extended in vivo observation and ex vivo

characterization. Most studies follow the method of Hnatowich et al. [108], which modifies HDL [109] or LDL [100, 110–113] with the chelator diethylenetriamine-pentaacetic acid (DTPA), followed by radiolabeling with [ $^{111}\text{In}$ ]InCl<sub>3</sub>. 2,2',2'',2'''-(1,4,7,10-tetraazacyclododecane-1,4,7,10-tetrayl)tetraacetic acid (DOTA, Fig. 2C) has also been used as chelator for  $^{111}\text{In}$  to label the apolipoprotein components of HDL and LDL [114]. Alternatively, LDL's lipids can be  $^{111}\text{In}$ -labeled using the hydrophobic chelator DTPA-bis(stearylamide) [62].

Perez-Medina et al. developed similar methods to radiolabel rHDL with  $^{89}\text{Zr}$  ( $t_{1/2} = 3.2$  d) to facilitate in vivo PET imaging studies over several days [115, 116]. Specifically, the phospholipid 1,2-distearoyl-*sn*-glycero-3-phosphorylethanolamine (DSPE) was functionalized with the chelator deferoxamine B (DFO, Fig. 2C) and formulated into rHDL to enable chelation of  $^{89}\text{Zr}$  [66, 68, 115, 117]. These authors also developed a hydrophobic DFO chelator (C<sub>34</sub>-DFO) to label the core of drug-loaded rHDL formulations [118], and labeled rHDL post-formulation by functionalizing its apolipoprotein component with DFO [21, 88, 119]. Zr-DFO radiochemistry is highly suitable for labeling (lipo)proteins as it requires a mild pH of  $\sim 7$ , a relatively low temperature (typically 37 °C), and a short reaction time (30–60 min). However,  $^{89}\text{Zr}$  release from DFO is a concern in vivo, especially over long observation periods, leading to high bone uptake due to this radioisotope's affinity for phosphates. The poor solubility of DFO can also result in the formation of DFO-aggregates upon lipoprotein functionalization, which are difficult to detect if quality control is based on thin layer chromatography [120]. These issues have prompted research toward developing  $^{89}\text{Zr}$  ligands with improved chelating properties [121]. Other radiometals used for lipoprotein radiolabeling are  $^{68}\text{Ga}$  ( $t_{1/2} = 68$  min), to label DTPA-functionalized LDL [100], and  $^{59}\text{Fe}$  ( $t_{1/2} = 44.6$  d), which can be included as part of a superparamagnetic iron oxide core [122].

### Tritium and other radionuclides

Tritium ( $^3\text{H}$ ,  $t_{1/2} = 12.3$  y) has historically been the most frequently used radionuclide for lipoprotein labeling. The majority of applications employed tritiated cholesterol derivatives that naturally embed in lipoproteins, including [ $^3\text{H}$ ]cholesterol (Fig. 2D) [38, 73, 123], [ $^3\text{H}$ ]cholesteryl esters [38, 73, 98, 123], or [ $^3\text{H}$ ]cholesteryl oleyl ether [38, 95, 98, 124–126]. The tritiated triglyceride [ $^3\text{H}$ ]triolein was similarly used to label reconstituted HDL [127]. Radiolabeling of lipoproteins' apolipoprotein components has also been achieved in cultured cells using tritiated amino acids [73, 128, 129], and in squirrel monkeys and rabbits through [ $^3\text{H}$ ]leucine or [ $^3\text{H}$ ]cholesterol administration [97, 130]. Analogously, carbon-14 ( $^{14}\text{C}$ )-labeled cholesterol

(Fig. 2D) derivatives and phospholipids have been used for HDL labeling [127, 131]. Some of these studies followed a dual labeling approach, where a [ $^3\text{H}$ ]- or [ $^{14}\text{C}$ ]-labeled cholesterol derivative was used in combination with radioiodination of the protein component [73, 98, 124, 131].  $^3\text{H}$  or  $^{14}\text{C}$  advantageously allow radiolabeling by creating isotopologues, meaning that the structure and biological behavior of the labeled molecules remain largely unaltered. More recently, methods to label lipoproteins with the PET isotope fluorine-18 ( $^{18}\text{F}$ ,  $t_{1/2} = 109$  min) have been reported. Pietzsch et al. [132] devised an analogous strategy to the Bolton-Hunter radioiodination method to couple  $^{18}\text{F}$  to LDL and oxLDL, using the activated ester *N*-succinimidyl-4- $^{18}\text{F}$ fluorobenzoate. This isotope was also incorporated into the lipid core of chylomicrons as a [ $^{18}\text{F}$ ]-4,4-difluoro-4-bora-3a,4a-diaza-s-indacene (BODIPY)-triglyceride [133].

## Studying lipoprotein biology by radiolabeling

### Studying lipoprotein metabolism in vivo

In 1975, Barry Lewis et al. investigated the kinetic relationship between VLDL and LDL by injecting  $^{131}\text{I}$ -labeled VLDL in humans and tracked radioactivity levels in the LDL fraction of plasma samples [40]. Results showed that the  $^{131}\text{I}$  was associated with the apolipoprotein B (apoB) component of VLDL, and the decline of the specific activity curve of apoB in VLDL intersected with the maximal height of the LDL-apoB curve, indicating a precursor-product relationship. Mathematical modeling revealed that approximately 90% of VLDL-apoB mass was converted to LDL-apoB, and that most, if not all, LDL-apoB derived from VLDL-apoB. These were crucial observations, as it remained unknown whether LDL production was direct, or indirect through the conversion of VLDL.

Building on this work, Virgil Brown et al., in 1982, examined the factors that contribute to the conversion of VLDL into LDL [42]. In non-human primates, using both  $^{125}\text{I}$ - and  $^{131}\text{I}$ -labeled VLDL, in combination with an inhibitor of hepatic lipase, they showed that the conversion of VLDL and IDL to LDL was delayed. Taking into account other work on lipoprotein lipase [134], the authors concluded that both lipolytic enzymes function in parallel to convert triglyceride-rich VLDL to triglyceride-depleted IDL and finally to triglyceride-poor LDL.

Also in the early 1980's, there was interest in the roles of other apolipoproteins than apoB in VLDL and LDL metabolism. Interest in apoE, a known VLDL-associated apolipoprotein, in particular, was increased with the recognition that three isoforms of this protein exist [135], namely E2,

E3, E4 [136, 137]. The roles of these isoforms in plasma VLDL clearance were studied in subjects with normo- or hyperlipidemia. For example, H. Bryan Brewer et al. radiolabeled the most common isoform of apoE, E3, with  $^{131}\text{I}$ , and then allowed it to associate with human VLDL isolated from normolipidemic human subjects. This reconstituted VLDL was injected into subjects, and the distribution of the radiolabeled apoE among the lipoprotein fractions and its clearance from plasma were studied. Results showed that apoE is crucial for clearing triglyceride-rich VLDL. In contrast with hepatic lipase and lipoprotein lipase, which hydrolyze triglycerides in VLDL and IDL, this and related studies established apoE as a ligand mediating the clearance of these lipoproteins, particularly by the liver. Subsequent studies of the other apoE isoforms showed that they impact the clearance of triglyceride-rich VLDL particles, likely due to differential binding to the LDL receptor (apoE2, apoE3) or the interference in lipolytic processing of VLDL (apoE4) [137].

Our understanding of HDL metabolism has also benefited from radiolabeling. In humans, HDL has two major protein constituents, apoA1 and apoA2. Some HDL particles have both proteins, and some have only apoA1. In a series of studies, these proteins were labeled *ex vivo* with  $^{125}\text{I}$ , injected into human subjects, and plasma samples taken at various time points [138]. The results showed that the radiolabeled apolipoproteins rapidly associate with circulating HDL, and that the plasma half-life of radiolabeled HDL is 5.8 days. The rate of HDL protein synthesis was estimated to be 8.51 mg/kg per day. In an extension of this kinetic study, investigators wondered whether HDL particles containing apoA1 only (HDL-A1) or apoA1 and apoA2 (HDL-A1/A2) differed in their metabolism, a question that could not be resolved in the previous study as both proteins were identically radiolabeled [44]. Thus, the authors radiolabeled purified apoA1 with  $^{125}\text{I}$  and apoA2 with  $^{131}\text{I}$  and reassociated them with autologous HDL, which was then injected into human subjects. After isolating HDL-A1 and HDL-A1/A2 from plasma at various time points, kinetic analysis showed that HDL-A1 has a shorter plasma residence time than HDL-A1/A2 (4.39 vs. 5.17 days). These findings indicate that HDL subtypes have divergent metabolic pathways, and likely different functions in human metabolism.

Radiolabeling has also enabled studying how dietary factors influence lipoprotein metabolism. In pioneering studies reported by Shepard and colleagues in 1980 [139], the investigators showed the first evidence that dietary saturated fatty acids elevate LDL levels in human subjects by decreasing the plasma clearance of  $^{131}\text{I}$ -LDL. This clinical study was one of many using radioisotopes to determine the kinetic effects of dietary factors (*e.g.*, specific fatty acids, carbohydrate or protein content and composition), on the protein and lipid components of the major lipoprotein classes [140].

Important findings from these studies include that saturated fatty acids raise LDL levels by decreasing their plasma clearance, *trans*-fatty acids do the same but also increase HDL-apoA1 clearance, or that the n-3 fatty acids found in fish oils reduce VLDL-apoB production and promote VLDL conversion to smaller particles. In this context, it is interesting that the Mediterranean diet reduces LDL plasma levels by boosting its plasma clearance. These findings have been very influential in developing ‘heart-healthy diets’ by the American Heart Association [141] and the ban of *trans*-fatty acids from New York City restaurants [142].

### In vitro and in vivo studies on lipoprotein-cell interactions

The classic studies of Michael Brown and Joseph Goldstein that identified and characterized the LDL receptor relied heavily on radiolabeled LDL in an extensive series of papers. In 1974, the authors used  $^{125}\text{I}$ -LDL to show that in fibroblasts from a healthy subject, LDL bound in a high affinity, saturable manner, consistent with there being a specific receptor [143]. Notably, these binding characteristics were absent in cells from a homozygous familial hypercholesterolemia donor, with subsequent work showing that these lacked functional LDL receptors [144]. Furthermore, the fate of the  $^{125}\text{I}$ -LDL protein (*i.e.*, apoB) in the cell was an early and crucial piece of evidence for what became known as the receptor-mediated endocytosis pathway.

Radiolabeling approaches have also contributed to studies on the cellular interactions of HDL. It is well-known that HDL accepts excess cellular cholesterol through interactions with the ABCA1 and ABCG1 plasma membrane proteins [17]. HDL then delivers this cholesterol to the liver, from which it can be eliminated in various ways, but HDL itself is not taken up. This process has been termed reverse cholesterol transport (RCT) [17]. The molecular basis for RCT remained largely unknown until the seminal studies of Krieger and colleagues. There was reason to suspect the scavenger receptor SR-B1, cloned in 1994 by this group, was integral to the RCT process. In 1996, this suspicion became a reality due to a series of *in vitro* experiments using HDL in which the protein and lipid components were both radiolabeled [46].

In a series of elegant tissue culture studies, the same authors showed that  $^{125}\text{I}$ -HDL protein bound with high affinity and specificity to SR-B1, and while the  $^3\text{H}$ -cholesteryl ester that it carried was taken up by the cells, the  $^{125}\text{I}$ -labeled fraction was not. Later it was shown that SR-B1 is also responsible for *in vivo* HDL cholesteryl ester uptake by the liver [145]. Rinninger et al. similarly doubly-radiolabeled HDL ( $^{125}\text{I}$ -HDL protein and  $^3\text{H}$ -HDL cholesteryl ester) and injected it into mice sufficient or deficient in SR-B1. In the sufficient mice, the plasma disappearance of labeled

cholesteryl ester was faster than the protein. The liver uptake of  $^3\text{H}$ -cholesteryl ester was also higher than that of  $^{125}\text{I}$ -HDL protein. These results are consistent with the selective uptake observed in tissue culture. Taken together, these papers show that SR-B1 mediates selective uptake of HDL cholesteryl esters in vitro and in vivo. Besides giving insight into the mechanisms of RCT, these results spurred many other studies in vitro and in vivo, including of subjects with SR-B1 mutations [146].

Radiolabeling of lipoproteins also helped show that besides HDL being a vital ligand for SR-B1, VLDL remnants, *i.e.*, VLDL that have triglyceride content removed by lipases, also bind SR-B1 [147]. In these studies, Van Berkel et al. radiolabeled VLDL remnants with  $^{125}\text{I}$  and injected them into mice that were wild type (*i.e.*, sufficient) or deficient in SR-B1. Radioactivity uptake by the liver was  $\sim 3$  times greater in the SR-B1 sufficient versus deficient mice. In studies in vitro, hepatocyte binding experiments showed high affinity binding of  $^{125}\text{I}$ -labeled VLDL remnants only in the SR-B1 sufficient mice.

## Studying disease using radiolabeled lipoproteins

### Studying disease mechanisms

Nuclear techniques have helped unravel the interplay between diseases and lipoprotein composition, behavior, and metabolism. For instance, in atherosclerosis, cholesterol efflux assays have shown how HDL transports cholesterol from plaques and peripheral tissues to the liver [148, 149]. These in vitro assays involve incubating macrophages with radioactive lipids, *e.g.*, [ $^3\text{H}$ ]cholesterol, before exposing the cells to apoB-depleted serum, which largely lacks lipoproteins except HDL. Cholesterol efflux can then be assessed by determining the radioactivity of the cells or medium [150]. The impact of lipoprotein composition or certain cellular pathways on cholesterol efflux can similarly be studied by varying the lipoprotein used or co-incubating inhibitors [148, 151]. Still, studies indicate that much of the radiolabeled cholesterol released from macrophages in such assays accumulates on albumin rather than inside lipoproteins. Furthermore, a paradoxical enhanced prospective risk of cardiovascular disease for people whose serum showed heightened cholesterol efflux activity exists [149]. Therefore, the outcomes of cholesterol assays should be interpreted with care.

Radiolabeled lipoproteins have also expanded understanding of scavenger receptors in atherosclerosis. Ishibashi et al. labeled lipoproteins with  $^{125}\text{I}$  and they observed significantly longer VLDL and LDL blood half-lives in LDL receptor (LDLr) deficient (*Ldlr*<sup>-/-</sup>) versus wild type (WT)

mice, while HDL blood half-lives were similar across strains (Fig. 3A) [152]. These results helped demonstrate that the LDLr mediates the uptake of VLDL and LDL, but not HDL. In a similar study, Huszar et al. observed lower LDL levels in *Ldlr*<sup>-/-</sup> mice compared to *Ldlr*<sup>-/-</sup> mice that also displayed attenuated SR-B1 expression [153]. The authors then used radiolabeled LDL to show that LDL blood clearance and liver uptake were similar between the groups, indicating that SR-B1 depletion increases LDL production, rather than decreasing its catabolism. A similar study revealed that SR-B1 regulates the uptake of pro-atherogenic Lp(a) [154].

Besides atherosclerosis, other cardiometabolic conditions have also been studied by radiolabeling lipoproteins. Hypoxia following myocardial infarction promotes cardiac dysfunction by increasing lipid accumulation in the heart. To study this, VLDL containing a  $^3\text{H}$ -labeled cholesteryl ester ( $^3\text{H}$ -CE) and  $^{14}\text{C}$ -labeled triglyceride ( $^{14}\text{C}$ -TG) was used to study lipid uptake by HL-1 cardiomyocytes under normoxia and hypoxia conditions in vitro [155]. The authors found that hypoxia significantly increased  $^3\text{H}$ -CE uptake by HL-1 cells and that inhibiting low-density lipoprotein receptor-related protein 1 (LRP1) prevents this (Fig. 3B). Interestingly, hypoxia similarly increased  $^{14}\text{C}$ -TG uptake but it could not be reduced by LRP1 inhibition. Hence, these results indicate that LRP1 regulates the uptake of cholesteryl esters but not triglycerides, a finding that has spurred efforts to promote myocardial infarction recovery by inhibiting LRP1 [158].

Radiolabeling has also illuminated how diabetes alters lipoprotein behavior [159, 160] and metabolism [156, 161]. For instance, Niu et al. studied the myocardial metabolism of lipoproteins in the ZDF rat model of early-onset type 2 diabetes [156]. The authors perfused working hearts from healthy and diabetic rats *ex vivo* with VLDL containing a  $^3\text{H}$ -labeled triacylglyceride ( $^3\text{H}$ ]TAG-VLDL), and they determined heart triacylglyceride utilization rates, defined as the total amount of triglyceride that was oxidized, by quantifying  $^3\text{H}_2\text{O}$ , or incorporated into tissue lipids, by determining tissue lipid  $^3\text{H}$  levels. The results revealed that hearts perfused with VLDL obtained from diabetic rats consume more triacylglycerides, primarily by oxidation (Fig. 3C-D). In line, the authors perfused the hearts with [ $^{14}\text{C}$ ]glucose and found that diabetic hearts display significantly less glucose oxidation, indicating a shift from glycolysis to fatty acid metabolism (Fig. 3E). An increased lipid accumulation in the heart has also been observed in diabetic patients and at least partly underlies the lipotoxicity and cardiac dysfunction observed in such people [162–164].

Tangier disease is characterized by an accumulation of lipids in peripheral tissues, but the underlying mechanisms were long unknown [165, 166]. Cholesterol efflux assays using radiolabeled cholesterol or apolipoproteins have revealed that apoA1 and HDL are impaired in mediating

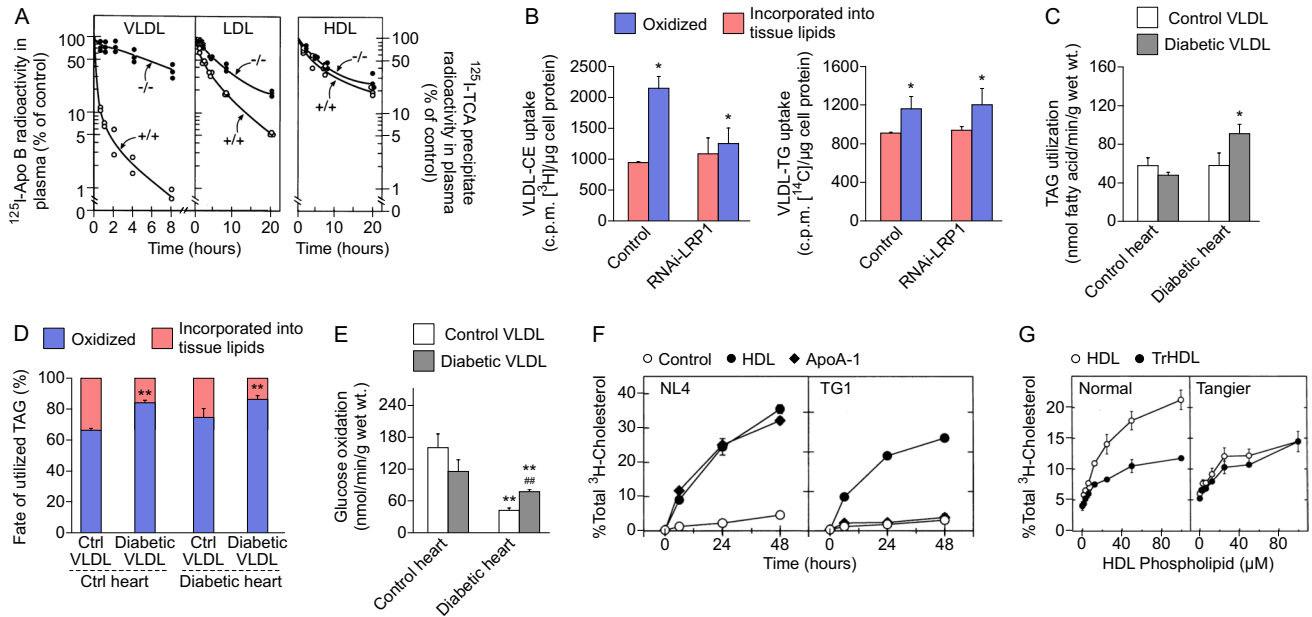


**Fig. 3** **A**)  $^{125}\text{I}$ -labeled lipoproteins were *i.v.* administered to wild type (open dots) or *Ldlr*<sup>-/-</sup> (closed dots) mice and plasma radioactivity monitored over time,  $n = 3$  [152]. **B**) Under normoxic or hypoxic conditions, HL-1 cells were incubated with VLDL containing  $^3\text{H}$ -labeled cholesteryl ester (left) or  $^{14}\text{C}$ -labeled triglyceride (right) and lipid uptake determined by measuring the radioactivity of cell homogenates,  $n = 3$  [155]. **C–E**) Hearts from healthy rats or a rat diabetes model were perfused with VLDL from either group. Loading the VLDL with a [ $^3\text{H}$ ]-labeled triacylglyceride ( $^3\text{H}$ ]TAG-VLDL) enabled radioactivity assays to determine **C**) triglyceride utilization, defined as the sum of **D**) triglyceride oxidation and the amount of triglycerides incorporated into tissue lipids. **E**) [ $^{14}\text{C}$ ]glucose was used to determine the hearts' glucose oxidation rate. Significant differ-

ences are denoted as follows: for panel B, differences between control hearts are indicated as  $*p < 0.05$ ; for panels C and D, differences between control VLDL-treated and control hearts are indicated as  $**p < 0.01$ , and differences between control VLDL-treated diabetic hearts as  $###p < 0.01$ ,  $n = 7$  [156]. **F**) [ $^3\text{H}$ ]cholesterol efflux from normal (NL4) or Tangier fibroblasts (TG1) in the presence of albumin only (control) or albumin and HDL or apoA-I,  $n = 3$  [157]. **G**) [ $^3\text{H}$ ]cholesterol was incubated for 72 h with NL4 or TG1 in the presence of the ACAT inhibitor 58.035, which prevents cholesterol esterification. Next, different amounts of normal or trypsin-treated HDL (TrHDL) were added and cholesterol efflux quantified four hours later,  $n = 3$  [157]

cholesterol efflux from fibroblasts obtained from Tangier patients (Fig. 3F) [157, 167, 168]. Interestingly, similar experiments using LDL did not show significant differences between healthy persons and Tangier patients [169]. To study this more thoroughly, the cholesterol efflux by normal versus trypsin-treated HDL (TrHDL) was compared [157]. Trypsin impairs HDL's ability to remove intracellular cholesterol but does not affect its propensity to remove plasma membrane cholesterol. Results showed that the cholesterol efflux from healthy fibroblasts is lower when using TrHDL versus normal HDL, but that this difference disappears when using Tangier fibroblasts, indicating that Tangier disease affects HDL's ability to remove plasma membrane cholesterol (Fig. 3G). Similar studies using  $^{14}\text{C}$ -labeled cholesterol and the sterol precursor [ $^{14}\text{C}$ ]mevalonolactone revealed that the dysfunctional cholesterol efflux in Tangier results from impaired HDL-mediated activation of protein kinase C (PKC) [169]. It is now known that these differences between Tangier patients and healthy individuals stem from mutations in the *ABCA1* gene [170].

## Imaging radiolabeled lipoproteins for diagnostic purposes

Nuclear imaging enables diagnosing disease by monitoring the abundance and dynamics of radiolabeled lipoproteins. Radiolabeled lipoproteins have been extensively used to evaluate plaque size and distribution in atherosclerosis [115, 171, 172]. For instance, Yong-Sang et al. radiolabeled HDL by inserting a  $^{68}\text{Ga}$ -lipid-chelator conjugate and administered this to atherosclerotic apoE deficient (*ApoE*<sup>-/-</sup>) mice or naïve C57BL/6 controls [173]. Subsequent PET imaging showed that the  $^{68}\text{Ga}$ -labeled HDL effectively accumulates in atherosclerotic plaques (Fig. 4A). Still, small animal models do not fully recapitulate human atherosclerosis and the small size of mouse blood vessels complicates plaque imaging. Therefore, radiolabeled lipoproteins were used to study atherosclerotic plaques in pigs [116]. Specifically,  $^{89}\text{Zr}$  and the chelator DFO were used to radiolabel HDL's phospholipids ( $^{89}\text{Zr}$ -PL-HDL). These nanoparticles were administered to a swine model of familial hypercholesterolemia, in which plaque development was promoted by injuring the femoral

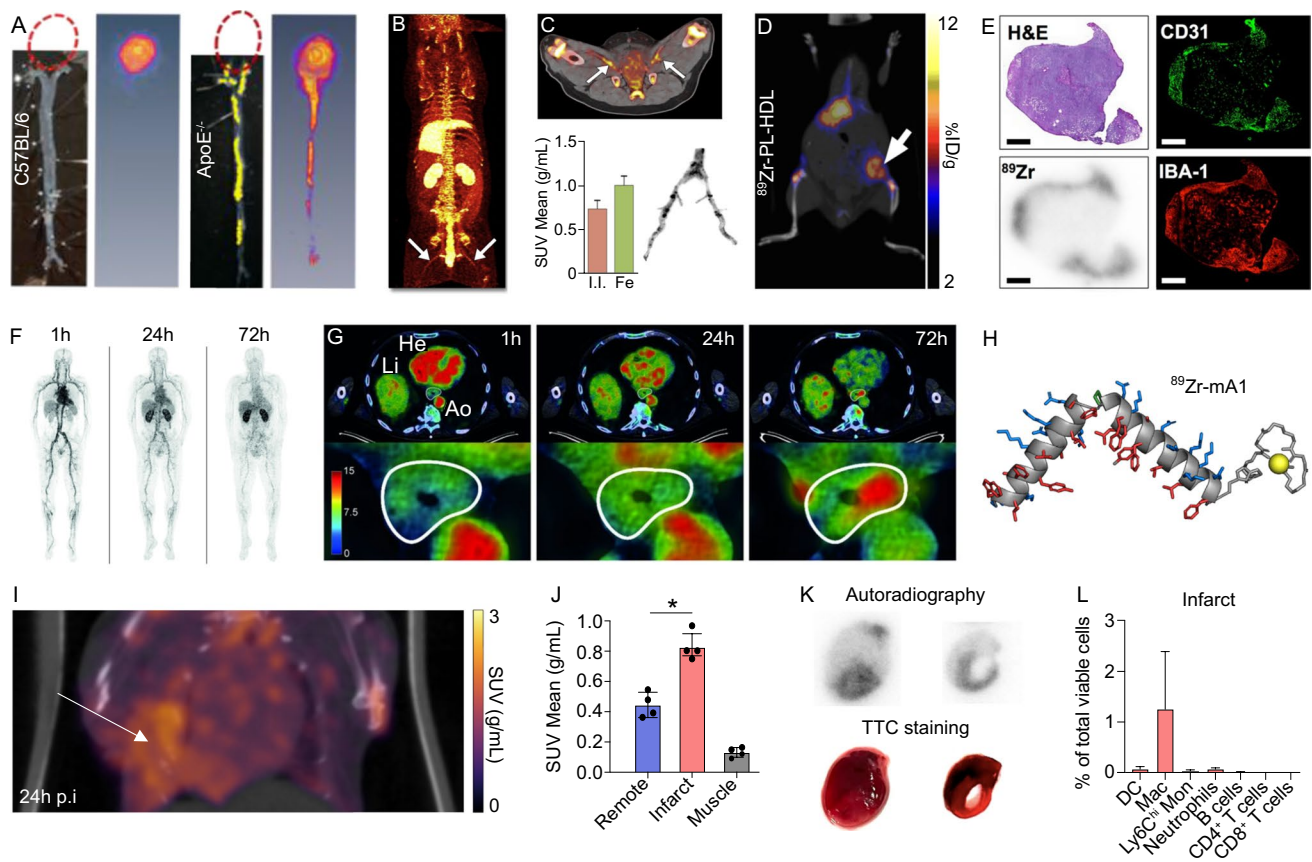


**Fig. 4** A) Macroscopic view and 3D PET images of the aortas of C57BL/6 and *ApoE*<sup>-/-</sup> mice *i.v.* injected with <sup>68</sup>Ga-labeled HDL. Red circle indicates the prior location of the heart [173]. B-C) A swine model of atherosclerosis was *i.v.* injected with <sup>89</sup>Zr-labeled HDL and analyzed 48 h later. B) Whole-body maximum intensity projection of PET signal intensity. Arrows indicate atherosclerotic femoral arteries. C) Axial PET image showing higher uptake in the femoral arteries (Fe) than the internal iliac (I.I.) control, *n* = 3. A representative autoradiograph of the femoral arteries is also shown [116]. D-E) An orthotopic 4T1 breast cancer mouse model was established, eight days later *i.v.* injected with <sup>89</sup>Zr-PL-HDL, and analyzed 24 h later. D) PET/CT image, arrows indicate the tumor. E) Ex vivo analysis of the tumors, showing clockwise starting from the top left, hematoxylin and eosin staining, CD31 staining for endothelial cells, IBA-1 staining for macrophages, and an autoradiograph showing radioactivity distribution. Scale bar = 2 mm [115]. F-G) <sup>89</sup>Zr-labeled CER-001 was used to image esophageal cancer in patients. F) Whole-body maximum-intensity projections at different time points post-injection. G)

Axial images, white lines denote the esophagus. Ao, aorta; He, heart; Li, liver [70]. H-L) An apoA1 mimetic peptide was labeled with <sup>89</sup>Zr to create <sup>89</sup>Zr-mA1 and evaluated this radiotracer's applicability to monitor inflammation in a mouse model of myocardial infarction by left anterior descending artery ligation [175]. H) Conformation of <sup>89</sup>Zr-mA1 as determined by AlphaFold. I) <sup>89</sup>Zr-mA1 was *i.v.* administered two days after MI and the animals PET/CT imaged one day later, *n* = 4. J) <sup>89</sup>Zr-mA1 uptake based on the PET data, *n* = 4. K) The heart was imaged by autoradiography, showing the whole heart followed by a representative 1 mm thick slice. TTC-staining of the tissues is also shown, revealing that the radiotracer accumulated in the infarcted area. L) mA1 was labeled with 'cold' <sup>nat</sup>Zr and administered this two days after MI. One day later, the infarct was analyzed by CyTOF to determine the percentage of the total viable cells that are <sup>nat</sup>Zr.<sup>+</sup> and of a certain cell type, *n* = 3. DC, dendritic cells; Mac, macrophages; Mon, monocytes; remote, remote myocardium. \**P* < 0.05

arteries using balloons. Two days later, the animals were analyzed by PET imaging, revealing substantially more tracer in the femoral arteries compared to the atherosclerosis-free internal iliac arteries (Fig. 4B-C). Inspired by these results, investigators from the Amsterdam University Medical Center used an <sup>89</sup>Zr-labeled analog of the HDL mimetic CER-001 to image atherosclerotic plaques in patients [174].

The overexpression of SR-B1, characteristic of certain types of tumors, also enables using radiolabeled lipoproteins to study cancer [62, 106]. <sup>89</sup>Zr-PL-HDL was used

to study the orthotopic 4T1 breast cancer mouse model, revealing that the tracer predominantly accumulates in tumor-associated macrophages (Fig. 4D-E) [115]. Such non-invasive insight into macrophage burden and dynamics could guide clinical breast cancer diagnosis and prognosis [176]. Analogous approaches using <sup>99m</sup>Tc-labeled HDL enabled imaging prostate cancer in a mouse model [106], and <sup>99m</sup>Tc-labeled LDL similarly facilitates studying melanoma-bearing mice [61]. Building on these

results, HDL-based PET imaging has recently been used to examine esophageal tumors in patients (Fig. 4F–G) [70].

Despite the diagnostic potential of radiolabeled lipoproteins, their clinical translation has been hindered by the challenges of producing GMP-grade reconstituted radiolabeled lipoproteins reproducibly and at scale. Therefore, several methods for radiolabeling endogenous lipoproteins *in vivo* have been developed. In one approach, radiolabeled lipids, such as [ $^3\text{H}$ ]oleic acid [177] or [ $^3\text{H}$ ]cholesterol [178] are *i.v.* administered, after which lipophilic interactions promote their incorporation into lipoproteins. In a similar approach, apolipoproteins are radiolabeled and allowed to bind lipoproteins *in vivo* [179, 180]. *In vivo* lipoprotein radiolabeling followed by *ex vivo* analysis enables studying differences in the natural behavior and catabolism of distinct lipoprotein subsets [180]. As isolating or expressing apolipoproteins is complex and expensive, a modified approach was developed in which  $^{89}\text{Zr}$  was used to radiolabel an apoA1-mimetic peptide ( $^{89}\text{Zr}$ -mA1) with lower molecular weight than endogenous apoA1 (~5.0 kDa versus 28 kDa), but similar lipoprotein affinity (Fig. 4H) [175, 181, 182]. After extensive *in vitro* validation of  $^{89}\text{Zr}$ -mA1's lipoprotein affinity, this probe was used to monitor myeloid cell dynamics in a mouse model of myocardial infarction (MI). Specifically, an MI by permanent LAD ligation was established and  $^{89}\text{Zr}$ -mA1 administered *i.v.* two days later. The following day, the animals were imaged *in vivo* by PET/CT, and radiotracer uptake was validated by *ex vivo* gamma counting, revealing high  $^{89}\text{Zr}$ -mA1 uptake in the infarcted area (Fig. 4I–J). Autoradiography and TTC-staining of whole hearts and 1-mm thick slices similarly showed increased radioactivity in the infarcted area compared to the remote myocardium (Fig. 4K). Next, mA1's cellular specificity was evaluated using a  $^{nat}\text{Zr}$ -labeled mA1 analog and its cellular uptake using CyTOF. Results showed that the majority of viable and  $^{nat}\text{Zr}$ -positive cells are macrophages, strongly suggesting that these predominantly underly PET signal intensity (Fig. 4L). Similar results were obtained in the B16F10 melanoma mouse model [175].

### Using radiochemistry to develop and guide lipoprotein-based therapies

HDL mediates reverse cholesterol transport and protects vascular endothelial cells as an antioxidant [183–185]. *In vivo*, people with low HDL cholesterol blood levels are at increased risk of atherosclerosis and MI [186, 187]. These beneficial effects of HDL have inspired attempts to reduce atherosclerosis and improve MI outcomes by infusing (reconstituted) HDL [188, 189]. PET and MR imaging have been used to quantify the carotid artery plaque uptake of HDL infusions, which might help guide these therapies' optimization and employment (Fig. 5A–C) [174]. Although

HDL infusions promote reverse cholesterol transport *in vivo*, clinical trials aimed at reducing atherosclerosis through this method have failed in the identification of significant health benefits, [190–192] perhaps because high HDL cholesterol levels can also increase cardiovascular disease risk [193, 194].

HDL's high biocompatibility and inherent propensity for uptake by phagocytes have encouraged their use as drug delivery vehicles. For instance, lipoproteins loaded or surface-functionalized with small molecule drugs [21, 22, 68, 197, 198], nucleic acids [195, 199–201], and proteins have been developed and employed [69]. Radiolabeling has been crucial in developing, applying, and translating these nanotherapeutics [202]. For instance, reconstituted lipoproteins containing a lipophilic peptidoglycan analog were developed and their potency in reducing melanoma tumor growth in mouse models demonstrated [22]. Radiolabeling these nanotherapeutics helped provide crucial insight into their uptake in the tumor and hematopoietic organs (Fig. 5D–E). Reconstituted lipoproteins loaded with siRNA have also been created and termed apolipoprotein lipid nanoparticles (aLNP) [203]. To study the *in vivo* integrity of these nanotherapeutics, the siRNA cargo was functionalized with DFO and radiolabeled with  $^{89}\text{Zr}$ , before formulating the resulting  $^{89}\text{Zr}$ -labeled siRNA into the lipoprotein nanocarrier. Next, either the bare or formulated  $^{89}\text{Zr}$ -labeled siRNA were *i.v.* administered to mice and imaged the animals by PET/CT 24 h later. The results revealed that bare siRNA predominantly accumulated in the kidneys, while lipoprotein-formulated siRNA ends up in the liver, demonstrating that the nanotherapeutic remains intact *in vivo* (Fig. 5F). The *in vivo* behavior of lipoprotein-based nanotherapeutics was similarly studied in other mouse models, rabbits, pigs, and non-human primates (Fig. 5G) [22, 68, 198, 204]. In an exciting but still largely unexplored approach, reconstituted lipoproteins were used for targeted alpha therapy by delivering the alpha emitter  $^{225}\text{Ac}$  to tumors overexpressing SR-B1 (Fig. 5H) [196]. The biodistribution of such lipoprotein-based alpha therapies could be imaged by substituting their alpha emitter with isotopes better suited for imaging, including  $^{132}\text{La}$ . [205] Overall, radiolabeling lipoprotein-based nanotherapeutics can improve preclinical studies and reduce patient risk by providing non-invasive, systemic, and quantitative insights into these therapeutics' *in vivo* behavior.

### Conclusion and outlook

The high sensitivity of radioactivity-based readouts and the non-invasive nature of nuclear imaging have made radiolabeling a highly effective strategy for studying lipoprotein behavior. Methods for radiolabeling lipoproteins by chelating or covalently binding various radionuclides have been

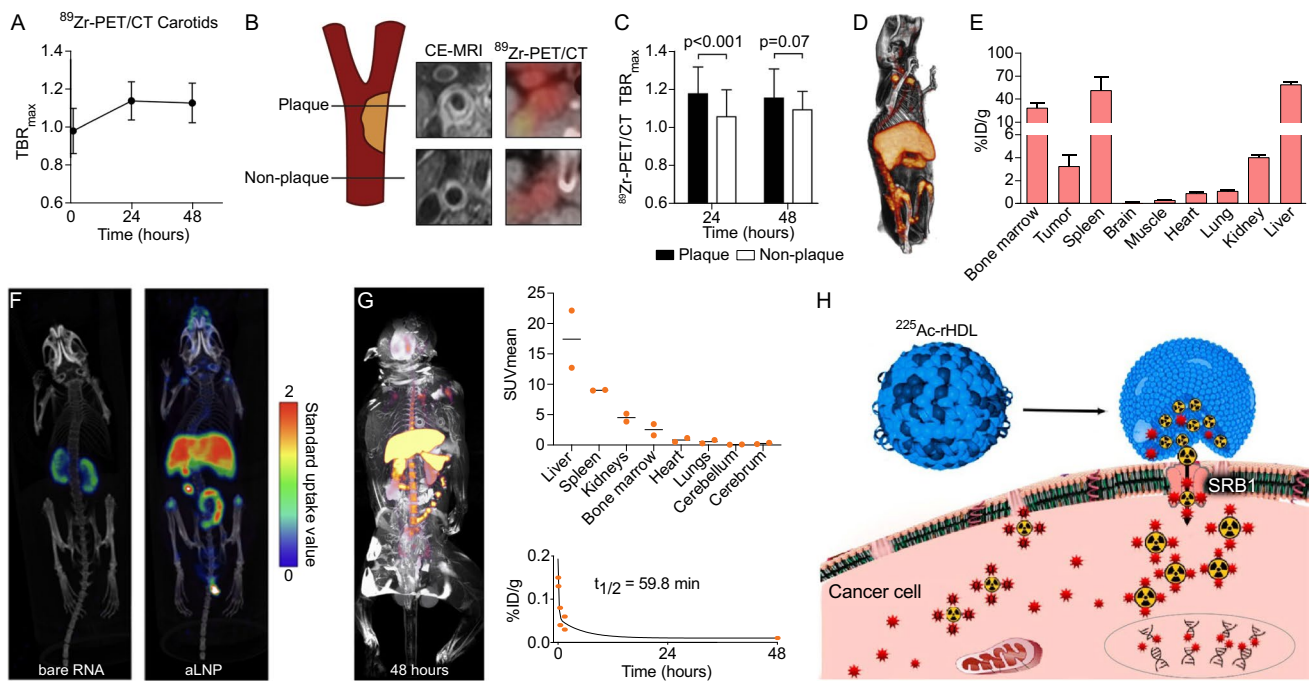


**Fig. 5** **A–C)** Patients with arteriosclerotic cardiovascular disease were *i.v.* injected with an  $^{89}\text{Zr}$ -labeled analog of the HDL mimetic CER-001. **A)** Carotid arteries-to-blood signal (target-to-background intensity,  $\text{TBR}_{\text{max}}$ ) over time as determined by PET/CT,  $n = 16$ . **B)** Representative contrast-enhanced (CE-)MRI and PET/CT images. **C)**  $\text{TBR}_{\text{max}}$  of plaque versus non-plaque carotid arteries 24 h post-injection,  $n = 18$  for both groups [174]. **D–E)** Reconstituted lipoproteins containing the peptidoglycan mimetic mifamurtide reduce melanoma tumor growth by inducing trained immunity. The nanotherapeutics were radiolabeled with  $^{89}\text{Zr}$ , administered *i.v.* to B16 F10 melanoma-bearing mice, and their biodistribution was studied 24 h later by D)

PET imaging and E) ex vivo gamma counting,  $n = 5$  [22]. **F)** Mice were administered *i.v.* with  $^{89}\text{Zr}$ -labeled siRNA or  $^{89}\text{Zr}$ -siRNA formulated into aLNPs, and imaged by PET/CT 24 h later [195]. **G)** A nonhuman primate was injected *i.v.* with  $^{89}\text{Zr}$ -labeled reconstituted HDL (rHDL)-based nanotherapeutics and imaged by PET/MRI 48 h later. Additionally, the therapeutic's blood half-life was determined by gamma counting blood aliquots,  $n = 2$  [21]. **H)** rHDL were loaded with the alpha emitter  $^{225}\text{Ac}$ . As the lipoprotein receptor SR-B1 is overexpressed in many tumors,  $^{225}\text{Ac}$ -rHDL predominantly accumulates in these cells, where the alpha radiation causes cell death [196]

developed, and these techniques have yielded valuable insights into lipoprotein stability, pharmacokinetics, and biodistribution in health and disease. Nonetheless, there are several limitations and issues to consider.

Most currently used radiolabeling approaches are non-specific and result in an irreproducible mixture of products, *e.g.*, variants in which different types of apolipoproteins or lipids are labeled. Improving techniques to functionalize predetermined lipoprotein components site-specifically will be crucial to studying their metabolism and kinetics. Related, the inherently dynamic nature of lipoproteins often means that varying results are obtained when radiolabeling different components [116, 119]. Repeating experiments while radiolabeling different lipoprotein constituents can help broaden the obtained insights. Alternatively, different lipoprotein components can be radiolabeled simultaneously using different radionuclides and distinguished by dual isotope nuclear imaging [206]. Related, the higher sensitivity and larger field-of-view of total-body PET scanners might benefit the *in vivo* study of rare lipoproteins and their constituents [207, 208].

Many mechanistic studies on lipoprotein biology have been performed *in vitro*, *e.g.*, by cholesterol efflux assays, which do not fully recapitulate the *in vivo* situation. Therefore, we recommend moving more lipoprotein studies *in vivo*, including accelerating the development of GMP-grade radiolabeled apolipoproteins and lipoproteins [70]. GMP-grade lipoproteins will similarly enable the clinical use of lipoprotein-based nanotherapeutics. rHDL and other reconstituted lipoproteins are well-tolerated as they consist entirely of endogenous compounds and mimic their natural analogs. For instance, CER-001 did not induce any signs of toxicity in human subjects at a dose of 16 g apoA-1/kg, roughly 60 times higher than the human equivalent dose of rHDL therapeutics effectively used in murine tumor models [209–211]. Rather, the broader clinical use of radiolabeled lipoproteins is limited by the challenges associated with the difficulty and cost of producing apolipoproteins at scale [203]. Apolipoproteins are typically isolated by ultracentrifugation of HDL concentrate [197] or obtained by recombinant expression [203]. Isolating apolipoproteins from blood is poorly scalable and introduces safety challenges, such as

the risk of retaining endotoxins. In contrast, recombinant proteins can be made in metric ton amounts [212]. Formulating large amounts of apolipoproteins and lipids into rHDL is already feasible by using a microfluidizer or an array of smaller microfluidic mixers [23]. The clinical use of rHDLs is also limited by their relatively poor reproducibility and high heterogeneity, which can complicate evaluating nanotherapeutics' in vivo behavior and comparing results across experiments or institutions [213]. Improved nanotherapeutic mixing and purification techniques are therefore highly needed [214].

Clinical trials employing lipoprotein-based therapeutics have focused on various conditions, including acute coronary syndrome, type 2 diabetes, atherothrombotic disease, acute coronary syndrome, and familial hypercholesterolemia [215]. Advancing these nanodrugs will require enhanced control over their stability, pharmacokinetics, and biodistribution. Although lyophilization allows stable storage of rHDLs for several years, their stability is much lower in the dynamic in vivo environment [216]. The shedding of (radiolabeled)lipids from lipoproteins can be decreased using lipids with longer aliphatic chains, fewer double bonds, and ether versus ester linkages [217]. Related, the blood half-life of HDL, typically around 48–72 h [215], can be controlled by varying its size, charge, and rigidity [218], potentially allowing for fewer therapeutic injections. Therapeutic rHDLs have also been directed to tissues of interest by incorporating different types of lipids and apolipoproteins [216] or functionalizing them with targeting ligands, including peptides and antibodies [215, 219–221].

Although radiolabeling has been invaluable for evaluating and optimizing the in vivo behavior of lipoproteins and lipoprotein-based therapeutics, employing radioactivity in humans comes with technical challenges and an inherent risk. Therefore, ex vivo mass spectrometry in conjugation with stable isotope lipoprotein labeling, such as using  $^{13}\text{C}$  and  $^{15}\text{N}$ , is increasingly used [222]. In contrast to most radionuclide-based methods, stable isotope labeling of lipoprotein is typically performed endogenously, *i.e.*, isotopically-labeled amino acids are administered and these then incorporate into (apo)lipoproteins in the normal course of their in vivo synthesis. Interestingly, studies comparing the kinetics of lipoproteins labeled endogenously using stable isotopes versus those labeled ex vivo (*i.e.*, exogenously) by radiolabeling have revealed differences, which may reflect post-translationally or artificially introduced modifications. Although monitoring stable isotopes by ex vivo mass spectrometry enables the simultaneous monitoring of multiple lipoprotein components, its invasiveness prevents the longitudinal and full-body studies made possible by the nuclear imaging of radiolabeled variants.

In summary, radiolabeling lipoproteins has contributed significantly to our understanding and management of

disease, and continued advances in (apo)lipoprotein isolation and synthesis, radiolabeling, and nuclear imaging guarantee a bright future for this approach.

**Author contributions** WJMM and AJPT contributed to the review's conception and design. All authors contributed to the draft and read and approved the final manuscript.

**Funding** WJMM, ZAF, and AJPT are supported by the United States National Institutes of Health grants no. 1P01 AI168258 -01 and 2P01HL131478 -06 A1.

**Data availability** Data sharing does not apply to this article as no datasets were generated during the current study.

**Declarations** We declare no competing interests. This article does not contain any new studies with human participants or animals performed by any of the authors.

**Ethics declarations** This is a systematic literature review; therefore, no ethical approval is required.

## References

- Walther TC, Farese RV. Lipid droplets and cellular lipid metabolism. *Annu Rev Biochem.* 2012;81:687–714.
- Harayama T, Riezman H. Understanding the diversity of membrane lipid composition. *Nat Rev Mol Cell Biol.* 2018;19:281–96.
- Wahli W, Michalik L. PPARs at the crossroads of lipid signaling and inflammation. *Trends Endocrinol Metab.* 2012;23:351–63.
- Rother N, et al. Acid ceramidase regulates innate immune memory. *Cell Rep.* 2023;42:113458.
- Randolph GJ, Miller NE. Lymphatic transport of high-density lipoproteins and chylomicrons. *J Clin Invest.* 2014;124:929–35.
- Jonas A, Phillips MC. Lipoprotein structure. *Biochemistry of lipids, lipoproteins and membranes.* Amsterdam: Elsevier Netherlands; 2008.
- Feingold KR, Grunfeld C. Introduction to lipids and lipoproteins. South Dartmouth: MDText.com, Inc; 2024.
- Yan J, et al. Dyslipidemia in rheumatoid arthritis: the possible mechanisms. *Front Immunol.* 2023;14:1254753.
- Mortensen MB, Nordestgaard BG. Elevated LDL cholesterol and increased risk of myocardial infarction and atherosclerotic cardiovascular disease in individuals aged 70–100 years: a contemporary primary prevention cohort. *The Lancet.* 2020;396:1644–52.
- Sharrett AR, et al. Coronary heart disease prediction from lipoprotein cholesterol levels, triglycerides, lipoprotein(a), apolipoproteins A-I and B, and HDL density subfractions: The Atherosclerosis Risk in Communities (ARIC) Study. *Circulation.* 2001;104:1108–13.
- Feig JE, et al. HDL promotes rapid atherosclerosis regression in mice and alters inflammatory properties of plaque monocyte-derived cells. *Proceed Natl Acad Sci.* 2011;108:7166–71.
- Glomset JA, Janssen ET, Kennedy R, Dobbins J. Role of plasma lecithin:cholesterol acyltransferase in the metabolism of high density lipoproteins. *J Lipid Res.* 1966;7:639–48.
- Weinstein DB, Carew TE, Steinberg D (1976) Uptake and degradation of low density lipoprotein by swine arterial smooth muscle cells with inhibition of cholesterol biosynthesis. *Biochimica et Biophysica Acta (BBA)-Lipids and Lipid Metabolism.* 424(3):404-21.

14. Levine DM, Parker TS, Donnelly TM, Walsh A, Rubin AL. In vivo protection against endotoxin by plasma high density lipoprotein. *Proc Natl Acad Sci*. 1993;90:12040–4.
15. Flegel WA, Baumstark MW, Weinstock C, Berg A, Northoff H. Prevention of endotoxin-induced monokine release by human low- and high-density lipoproteins and by apolipoprotein A-I. *Infect Immun*. 1993;61:5140–6.
16. Vickers KC, Palmisano BT, Shoucri BM, Shamburek RD, Remaley AT. MicroRNAs are transported in plasma and delivered to recipient cells by high-density lipoproteins. *Nat Cell Biol*. 2011;13:423–33.
17. Ouimet M, Barrett TJ, Fisher EA. HDL and Reverse Cholesterol Transport. *Circ Res*. 2019;124:1505–18.
18. Maran L, Hamid A, Bariyah S, Hamid S, Wertz PW. Lipoproteins as Markers for Monitoring Cancer Progression. *J Lipids*. 2021;2021:8180424.
19. McMahon KM, Plebanek MP, Thaxton CS. Properties of Native High-Density Lipoproteins Inspire Synthesis of Actively Targeted In Vivo siRNA Delivery Vehicles. *Adv Funct Mater*. 2016;26:7824–35.
20. Ng KK, Lovell JF, Zheng G. Lipoprotein-inspired nanoparticles for cancer theranostics. *Acc Chem Res*. 2011;44:1105–13.
21. van Leent MMT, et al. A modular approach toward producing nanotherapeutics targeting the innate immune system. *Sci Adv*. 2021;7:1–12.
22. Priem B, et al. Trained Immunity-Promoting Nanobiologic Therapy Suppresses Tumor Growth and Potentiates Checkpoint Inhibition. *Cell*. 2020;183:786–801.
23. Binderup T, et al. Imaging-assisted nanoimmunotherapy for atherosclerosis in multiple species. *Sci Transl Med*. 2019;11:7736.
24. Weissleder R, Mahmood U. Molecular imaging. *Radiology*. 2001;219:316–33.
25. Skajaa T, et al. High-density lipoprotein-based contrast agents for multimodal imaging of atherosclerosis. *Arterioscler Thromb Vasc Biol*. 2010;30:169–76.
26. Sabnis S, Sabnis NA, Raut S, Lacko AG. Superparamagnetic reconstituted high-density lipoprotein nanocarriers for magnetically guided drug delivery. *Int J Nanomedicine*. 2017;12:1453–64.
27. Nandwana V, et al. High-Density Lipoprotein-like Magnetic Nanostructures (HDL-MNS): Theranostic Agents for Cardiovascular Disease. *Chem Mater*. 2017;29:2276–82.
28. Barazza A, et al. The complex fate in plasma of gadolinium incorporated into high-density lipoproteins used for magnetic imaging of atherosclerotic plaques. *Bioconjug Chem*. 2013;24:1039–48.
29. Briley-Saebo KC, et al. High-relaxivity gadolinium-modified high-density lipoproteins as magnetic resonance imaging contrast agents. *J Phys Chem B*. 2009;113:6283–9.
30. Skajaa T, et al, Mulder WJ (2009) Nanotechnology in medical imaging: probe design and applications. *Arteriosclerosis, thrombosis, and vascular biology*. 29(7):992-1000.
31. Crich SG, et al. Magnetic Resonance Imaging Detection of Tumor Cells by Targeting Low-Density Lipoprotein Receptors with Gd-Loaded Low-Density Lipoprotein Particles. *Neoplasia*. 2007;9:1046–56.
32. Thaxton CS, Daniel WL, Giljohann DA, Thomas AD, Mirkin CA. Templated spherical high density lipoprotein nanoparticles. *J Am Chem Soc*. 2009;131:1384–5.
33. Massey JB, et al. Measurement and prediction of the rates of spontaneous transfer of phospholipids between plasma lipoproteins. *Biochimica et Biophysica Acta - Lipids and Lipid Metabolism*. 1984;794:274–80.
34. Melchior GW, Rudel LL. Heterogeneity in the low density lipoproteins of cholesterol fed African green monkeys (*Cercopithecus aethiops*). *Biochimica et Biophysica Acta - Lipids and Lipid Metabolism*. 1978;531:331–43.
35. Eisenberg S, Rachmilewitz D. Metabolism of rat plasma very low density lipoprotein: I fate in circulation of the whole lipoprotein. *Biochimica et Biophysica Acta (BBA)-Lipids and Lipid Metabolism*. 1973 Dec 20;326(3):378–90.
36. Ghiselli G, Krishnan S, Beigel Y, Gotto AM. Plasma metabolism of apolipoprotein A-IV in humans. *J Lipid Res*. 1988;27:813–27.
37. Van Berkel TJ, De Rijke YB, Kruijt JK. Different fate in vivo of oxidatively modified low density lipoprotein and acetylated low density lipoprotein in rats. Recognition by various scavenger receptors on Kupffer and endothelial liver cells. *J Biol Chem*. 1991;266(4):2282–9.
38. Stangl H, Hyatt M, Hobbs HH. Transport of lipids from high and low density lipoproteins via scavenger receptor-BI. *J Biol Chem*. 1999;274:32692–8.
39. Daerr WH, Pethke W, Windler ETE, Greten H (1990) Biotinyl-high-density lipoproteins as a probe for the determination of high-density lipoprotein turnover in humans. *Biochimica et Biophysica Acta (BBA) - Lipids and Lipid Metabolism* 1043, 311–317
40. Sigurdsson G, Nicoll A, Lewis B Conversion of very low density lipoprotein to low density lipoprotein A metabolic study of apolipoprotein B kinetics in human subjects. *J Clin Invest*. 1975;56:1481–90.
41. Kubow S. The influence of positional distribution of fatty acids in native, interesterified and structure-specific lipids on lipoprotein metabolism and atherogenesis. *J Nutr Biochem*. 1996;7:530–41.
42. Goldberg IJ, et al. Lipoprotein Metabolism during Acute Inhibition of Hepatic Triglyceride Lipase in the Cynomolgus Monkey. *J Clin Invest*. 1982;70:1184–92.
43. Gregg RE, Zech LA, Schaefer EJ, Brewer HB. Apolipoprotein E metabolism in normolipoproteinemic human subjects. *J Lipid Res*. 1984;25:1167–76.
44. Rader DJ, Castro G, Zech LA, Fruchart JC, Brewer HB. In vivo metabolism of apolipoprotein A-I on high density lipoprotein particles LpA-I and LpA-I. A-II *J Lipid Res*. 1991;32:1849–59.
45. De Rijke YB, Jurgens G, Hessels EMAJ, Hermann A, Van Berkel TJC. In vivo fate and scavenger receptor recognition of oxidized lipoprotein[a] isoforms in rats. *J Lipid Res*. 1992;33:1315–25.
46. Acton S, et al. Identification of scavenger receptor SR-BI as a high density lipoprotein receptor. *Science*. 1996;1979(271):518–20.
47. Huettinger M, et al. Imaging of hepatic low density lipoprotein receptors by radionuclide scintiscanning in vivo. *Proc Natl Acad Sci*. 1984;81:7599–603.
48. Morton RE, West GA, Hoff HF. A low density lipoprotein-sized particle isolated from human atherosclerotic lesions is internalized by macrophages via a non-scavenger-receptor mechanism. *J Lipid Res*. 1990;27:1124–34.
49. Tatò F, Vega GL, Tall AR, Grundy SM. Relation Between Cholesterol Ester Transfer Protein Activities and Lipoprotein Cholesterol in Patients With Hypercholesterolemia and Combined Hyperlipidemia. *Arterioscler Thromb Vasc Biol*. 1995;15:112–20.
50. Caslake MJ, et al. Fenofibrate and LDL metabolic heterogeneity in hypercholesterolemia. *Arterioscler Thromb*. 1993;13:702–11.
51. Ginsberg HN, Goldsmith SJ, Vallabhajosula S. Noninvasive imaging of 99mtechnetium-labeled low density lipoprotein uptake by tendon xanthomas in hypercholesterolemic patients. *Arteriosclerosis: An Official J Am Heart Assoc, Inc*. 1990 Mar;10(2):256-62.
52. Iuliano L, et al. Preparation and biodistribution of 99m technetium labelled oxidized LDL in man. *Atherosclerosis*. 1996;126:131–41.
53. Atsma DE, et al. Potential of 99mTc-LDLs labeled by two different methods for scintigraphic detection of experimental atherosclerosis in rabbits. *Arterioscler Thromb*. 1993;13:78–83.

54. Chang MY, Lees AM, Lees RS. Low-Density Lipoprotein Modification and Arterial Wall Accumulation in a Rabbit Model of Atherosclerosis. *Biochemistry*. 1993;32:8518–24.
55. Xiao W, Wang L, Scott T, Counsell RE, Liu H. Radiolabeled cholesteryl lopanoate/ acetylated low density lipoprotein as a potential probe for visualization of early atherosclerotic lesions in rabbits. *Pharm Res*. 1999;16:420–6.
56. An Official Journal of the American Heart Association. Lees, A. M. *et al.* Imaging human atherosclerosis with 99mTc-labeled low density lipoproteins. *Arteriosclerosis. Inc.* 1988;8:461–70.
57. Iuliano L, Mauriello A, Sbarigia E, Spagnoli LG, Violi F. Radiolabeled native low-density lipoprotein injected into patients with carotid stenosis accumulates in macrophages of atherosclerotic plaque: Effect of vitamin E supplementation. *Circulation*. 2000;101:1249–54.
58. Taylor AH, Stephan ZF, Steele RE, Wong NCW. Beneficial Effects of a Novel Thyromimetic on Lipoprotein Metabolism. *Mol Pharmacol*. 1997;52:542–7.
59. Bilheimer DW, Grundy SM, Brown MS, Goldstein JL. Mevinolin and colestipol stimulate receptor-mediated clearance of low density lipoprotein from plasma in familial hypercholesterolemia heterozygotes. *Proc Natl Acad Sci*. 1983;80:4124–8.
60. Chait A, Foster DM, Albers JJ, Failor RA, Brunzell JD. Low density lipoprotein metabolism in familial combined hyperlipidemia and familial hypercholesterolemia: Kinetic analysis using an integrated model. *Metabolism*. 1986;35:697–704.
61. Ponty E, Carton M, Soula G, Favre G, Benaniba R, Boneu A, Lucot H. Biodistribution study of 99mTc-labeled LDL in B16-melanoma-bearing mice Visualization of a preferential uptake by the tumor. *Int J Cancer*. 1993;54(3):411–7.
62. Jasanada F, et al. Indium-111 labeling of low density lipoproteins with the DTPA-Bis(stearylamide): evaluation as a potential radiopharmaceutical for tumor localization. *Bioconjug Chem*. 1996;7:72–81.
63. Monroe P, Vlahcevic ZR, Swell L. In vivo evaluation of lipoprotein cholesterol ester metabolism in patients with liver disease. *Gastroenterology*. 1983;85:820–9.
64. Thompson PD, et al. Effect of prolonged exercise training without weight loss on high-density lipoprotein metabolism in overweight men. *Metabolism*. 1997;46:217–23.
65. Vallabhajosula S, et al. Low density lipoprotein (LDL) distribution shown by 99mTechnetium-LDL imaging in patients with myeloproliferative diseases. *Ann Intern Med*. 1989;110:208–13.
66. Perez-Medina C, et al. Nanoreporter PET predicts the efficacy of anti-cancer nanotherapy. *Nat Commun*. 2016;7:1–8.
67. Senders ML, et al. Nanobody-Facilitated Multiparametric PET/MRI Phenotyping of Atherosclerosis. *JACC Cardiovasc Imaging*. 2019;12:2015–26.
68. Lameijer M, et al. Efficacy and safety assessment of a TRAF6-targeted nanoimmunotherapy in atherosclerotic mice and non-human primates. *Nat Biomed Eng*. 2018;2:279–92.
69. Schrijver DP, et al. Resolving sepsis-induced immunoparalysis via trained immunity by targeting interleukin-4 to myeloid cells. *Nature Biomed Eng*. 2023;2023:1–16.
70. Zheng KH, et al. 89Zr-labeled high-density lipoprotein nanoparticle pet imaging reveals tumor uptake in patients with esophageal cancer. *J Nucl Med*. 2022;63:1880–6.
71. McFarlane AS. Efficient Trace-labelling of Proteins with Iodine. *Nature*. 1958;182:53–53.
72. Huggins KW, et al. Dietary n-3 polyunsaturated fat increases the fractional catabolic rate of medium-sized HDL particles in African green monkeys. *J Lipid Res*. 2001;42:1457–66.
73. Jin FY, Kamanna VS, Kashyap ML. Niacin Decreases Removal of High-Density Lipoprotein Apolipoprotein A-I But Not Cholesterol Ester by Hep G2 Cells. *Arterioscler Thromb Vasc Biol*. 1997;17:2020–8.
74. Fainaru M, Glangeaud MC, Eisenberg S. Radioimmunoassay of human high density lipoprotein apoprotein AI. *Biochimica et Biophysica Acta (BBA)-Protein Structure*. 1975;386(2):432–43.
75. Vallabhajosula S, et al. Radiotracers for Low Density Lipoprotein Biodistribution Studies In Vivo: Technetium-99m Low Density Lipoprotein Versus Radioiodinated Low Density Lipoprotein Preparations. *J Nuc Med*. 1988;29:1237–45.
76. Moerlein SM, Dalal KB, Ebbe SN, Yano Y, Budinger TF. Residualizing and non-residualizing analogues of low-density lipoprotein as iodine-123 radiopharmaceuticals for imaging LDL catabolism International Journal of Radiation Applications and Instrumentation. Part B Nuclear Med Biol. 1988;15(2):141–9.
77. Roberts AB, et al. Selective accumulation of low density lipoproteins in damaged arterial wall. *J Lipid Res*. 1983;24:1160–7.
78. Bilheimer DW, Eisenberg S, Levy RI (1972) The metabolism of very low density lipoprotein proteins I Preliminary in vitro and in vivo observations. *Biochimica et Biophysica Acta (BBA)-Lipids and Lipid Metabolism*. 260(2):212–21.
79. Munford RS, Andersen JM, Dietsch JM. Sites of tissue binding and uptake in vivo of bacterial lipopolysaccharide-high density lipoprotein complexes: studies in the rat and squirrel monkey. *J Clin Invest*. 1981;68:1503–13.
80. Shepherd J, Patsch JR, Packard CJ, Gotto AM, Taunton OD. Dynamic properties of human high density lipoprotein apoproteins. *J Lipid Res*. 1978;19:383–9.
81. Bratzler RL, Chisolm GM, Colton CK, Smith KA, Lees RS. The distribution of labeled low-density lipoproteins across the rabbit thoracic aorta in vivo. *Atherosclerosis*. 1977;28:289–307.
82. Atsma DE, Kempen HJ, Nieuwenhuizen W, Van't Hooft FM, Pauwels EK. Partial characterization of low density lipoprotein preparations isolated from fresh and frozen plasma after radiolabeling by seven different methods. *J Lipid Res*. 1991;32(1):173–81.
83. Zhang B, Shimoji E, Tanaka H, Saku K. Evaluation of apolipoprotein A-I kinetics in rabbits in vivo using in situ and exogenous radioiodination methods. *Lipids*. 2003;38:209–18.
84. Huettinger M, et al. Imaging of hepatic low density lipoprotein receptors by radionuclide scintiscanning in vivo. *Proc Natl Acad Sci U S A*. 1984;81:7599–603.
85. Ramakrishnan R, Arad Y, Wong S, Ginsberg HN. Nonuniform radiolabeling of VLDL apolipoprotein B: implications for the analysis of studies of the kinetics of the metabolism of lipoproteins containing apolipoprotein B. *J Lipid Res*. 1990;31(6):1031–42.
86. Schonfeld G, Pflieger B. The Structure of Human High Density Lipoprotein and the Levels of Apolipoprotein A-I in Plasma as Determined by Radioimmunoassay. *J Clin Invest*. 1974;54:236–46.
87. Sobal G, Resch U, Sinzinger H. Modification of low-density lipoprotein by different radioiodination methods. *Nucl Med Biol*. 2004;31:381–8.
88. Shepherd J, Bedford DK, Morgan HG. Radioiodination of human low density lipoprotein: a comparison of four methods. *Clin Chim Acta*. 1976;66:97–109.
89. Greenwood FC, Hunter WM, Glover JS. The preparation of 131I-labelled human growth hormone of high specific radioactivity. *Biochem J*. 1963;89:114.
90. Marchalonis JJ. An enzymic method for the trace iodination of immunoglobulins and other proteins. *Biochem J*. 1969;113:299–305.
91. Romero JR, Martínez R, Fresnedo O, Ochoa B. Comparison of two methods for radioiodination on the oxidizability properties of low density lipoprotein. *J Physiol Biochem*. 2001;57:291–301.
92. Shaish A, Keren G, Chouraqui P, Levkovitz H, Harats D. Imaging of aortic atherosclerotic lesions by 125I-LDL, 125I-oxidized-LDL, 125I-HDL and 125I-BSA. *Pathobiology*. 2001;69:225–9.

93. Virgolini I, et al. Comparison of different methods for LDL isolation and radioiodination on liver LDL receptor binding in vitro. *Int J Rad Appl Instrum B*. 1991;18:513–7.
94. Salacinski PRP, McLean C, Sykes JEC, Clement-Jones VV, Lowry PJ. Iodination of proteins, glycoproteins, and peptides using a solid-phase oxidizing agent, 1,3,4,6-tetrachloro-3 $\alpha$ ,6 $\alpha$ -diphenyl glycoluril (Iodogen). *Anal Biochem*. 1981;117:136–46.
95. Julve J, et al. Mechanisms of HDL deficiency in mice overexpressing human apoA-II. *J Lipid Res*. 2002;43:1734–42.
96. Pittman RC, et al. A radioiodinated, intracellularly trapped ligand for determining the sites of plasma protein degradation in vivo. *Biochem J*. 1983;212:791–800.
97. Portman OW, Alexander M. Metabolism of [125I]tyramine cellobiose-labeled low density lipoproteins in squirrel monkeys. *Atherosclerosis*. 1985;56:283–99.
98. Rinninger F, et al. Lipoprotein lipase mediates an increase in the selective uptake of high density lipoprotein-associated cholesteryl esters by hepatic cells in culture. *J Lipid Res*. 1998;39:1335–48.
99. Lee JY, et al. HDLs in apoA-I transgenic Abca1 knockout mice are remodeled normally in plasma but are hypercatabolized by the kidney. *J Lipid Res*. 2005;46:2233–45.
100. Moerlein SM, Daugherty A, Sobel BE, Welch MJ. Metabolic Imaging with Gallium-68- and Indium-111-Labeled Low-Density Lipoprotein. *J Nucl Med*. 1991;32:300–7.
101. Daugherty A, Thorpe SR, Lange LG, Sobel BE, Schonfeld G. Loci of catabolism of beta-very low density lipoprotein in vivo delineated with a residualizing label, 125I-dilactitol tyramine. *J Biol Chem*. 1985;260:14564–70.
102. Bolton AE, Hunter WM. The labelling of proteins to high specific radioactivities by conjugation to a 125I-containing acylating agent. *Biochem J*. 1973;133:529–38.
103. Lees RS, Garabedian HD, Lees AM, Schumacher DJ, Miller A, Isaacsohn JL, Derksen A, Strauss HW. Technetium-99m Low Density Lipoproteins: Preparation and Biodistribution. *J Nucl Med*. 1985;26(9):1056–62.
104. Lees AM et al. Imaging human atherosclerosis with 99mTc-labeled low density lipoproteins. *Arteriosclerosis*. 1988;5:461–470.
105. Sobal G, Resch U, Tatzber F, Sinzinger H. Modification of low-density lipoprotein during radiolabeling with 99mTc using three labeling methods. *Quarter J Nucl Med Molec Imag*. 2006;50(4):333–43.
106. Isaac-Olivé K, et al. [99mTc-HYNIC-N-dodecylamide]: a new hydrophobic tracer for labelling reconstituted high-density lipoproteins (rHDL) for radioimaging. *Nanoscale*. 2019;11:541–51.
107. Pérez-Velasco DL, et al. Biokinetics, radiopharmacokinetics and estimation of the absorbed dose in healthy organs due to Technetium-99m transported in the core and on the surface of reconstituted high-density lipoprotein nanoparticles. *Nucl Med Biol*. 2023;122–123:1–12.
108. Hnatowich DJ, Layne WW, Childs RL. The preparation and labeling of DTPA-coupled albumin. *Int J Appl Radiat Isot*. 1982;33:327–32.
109. Virgolini I, et al. Binding of 111In-labeled HDL to platelets from normolipemic volunteers and patients with heterozygous familial hypercholesterolemia. *Arterioscler Thromb*. 1992;12:849–61.
110. Rosen JM, et al. Indium-111-labeled LDL: a potential agent for imaging atherosclerotic disease and lipoprotein biodistribution. *J Nucl Med*. 1990;31:343–50.
111. Leitha T, Staltdenherz A, Hermann M, Hottinger M, Gmeiner B. Parenchymal and nonparenchymal uptake of technetium-99m, indium-111, and iodine-125 low-density lipoprotein in the normal and estradiol-stimulated rat liver: tracer validation for quantitative low-density lipoprotein scintigraphy. *Hepatology*. 1995;22:1289–95.
112. Tietge UJF, et al. A sensitive noninvasive method for monitoring successful liver-directed gene transfer of the low-density lipoprotein receptor in Watanabe hyperlipidemic rabbits in vivo. *Gene Ther*. 2004;11:574–80.
113. Virgolini I, et al. Indium-111-Labeled Low-Density Lipoprotein Binds with Higher Affinity to the Human Liver as Compared to Iodine-123-Low-Density-Labeled Lipoprotein. *J Nucl Med*. 1991;32:2132–8.
114. Hadi T, et al. Lipoproteins LDL versus HDL as nanocarriers to target either cancer cells or macrophages. *JCI Insight*. 2020;5:1–14.
115. Perez-Medina C, et al. PET Imaging of Tumor-Associated Macrophages with 89Zr-Labeled High-Density Lipoprotein Nanoparticles. *J Nucl Med*. 2015;56:1272–7.
116. Pérez-Medina C, et al. In Vivo PET Imaging of HDL in Multiple Atherosclerosis Models. *JACC Cardiovasc Imaging*. 2016;9:950–61.
117. Pérez-Medina C, Fayad ZA, Mulder WJM. Atherosclerosis Immunoimaging by Positron Emission Tomography. *Arterioscler Thromb Vasc Biol*. 2020;40:865–73.
118. Tang J, et al. Immune cell screening of a nanoparticle library improves atherosclerosis therapy. *Proceed Natl Acad Sci*. 2016;113:6731–40.
119. Senders ML, et al. Probing myeloid cell dynamics in ischaemic heart disease by nanotracer hot-spot imaging. *Nat Nanotechnol*. 2020;15:398–405.
120. Wuensche TE, Lyashchenko S, van Dongen GAMS, Vugts D. Good practices for 89Zr radiopharmaceutical production and quality control. *EJNMMI Radiopharm Chem*. 2024;9:1–21.
121. Feiner IV, Brandt M, Cowell J, Demuth T, Vugts D, Gasser G, Mindt TL. The Race for Hydroxamate-Based Zirconium-89 Chelators. *Cancers*. 2021;13(17):4466.
122. Jung C, et al. Intraperitoneal injection improves the uptake of nanoparticle-labeled high-density lipoprotein to atherosclerotic plaques compared with intravenous injection: a multimodal imaging study in ApoE knockout mice. *Circ Cardiovasc Imaging*. 2014;7:303–11.
123. Masson D, Athias A, Lagrost L. Evidence for electronegativity of plasma high density lipoprotein-3 as one major determinant of human cholesteryl ester transfer protein activity. *J Lipid Res*. 1996;37:1579–90.
124. Brundert M, et al. Scavenger receptor CD36 mediates uptake of high density lipoproteins in mice and by cultured cells. *J Lipid Res*. 2011;52:745–58.
125. Singaraja RR, et al. Hepatic ATP-binding cassette transporter A1 is a key molecule in high-density lipoprotein cholesteryl ester metabolism in mice. *Arterioscler Thromb Vasc Biol*. 2006;26:1821–7.
126. Stein O, Halperin G, Stein Y. Biological labeling of very low density lipoproteins with cholesteryl linoleyl ether and its fate in the intact rat. *Biochim Biophys Acta*. 1980;620:247–60.
127. Kadowaki H, Patton GM, Robins SJ. Metabolism of high density lipoprotein lipids by the rat liver: evidence for participation of hepatic lipase in the uptake of cholesteryl ester. *J Lipid Res*. 1992;33:1689–98.
128. Edelstein C, et al. Comparative in vitro study of the pro-apolipoprotein A-I to apolipoprotein A-I converting activity between normal and Tangier plasma. *J Clin Invest*. 1984;74:1098–103.
129. Gordon JI, et al. Proteolytic processing of human preproapolipoprotein A-I A proposed defect in the conversion of pro A-I to A-I. in Tangier's disease. *J Biol Chem*. 1983;258:4037–44.
130. Portman OW, Illingworth DR, Alexander M (1975) The effects of hyperlipidemia on lipoprotein metabolism in squirrel monkeys and rabbits. *Biochimica et Biophysica Acta (BBA) - Lipids and Lipid Metabolism* 398, 55–71

131. Sasahara T, et al. The metabolic fate of apolipoprotein A-I-containing lipoproteins internalized into HepG2 cells: resecreted lipoproteins as a potent inducer for cholesterol efflux. *Atherosclerosis*. 1994;106:179–90.
132. Pietzsch J, et al. Fluorine-18 radiolabeling of low-density lipoproteins: a potential approach for characterization and differentiation of metabolism of native and oxidized low-density lipoproteins in vivo. *Nucl Med Biol*. 2004;31:1043–50.
133. Paulus A et al. (2019) [18F]BODIPY-triglyceride-containing chylomicron-like particles as an imaging agent for brown adipose tissue in vivo. *Scientif Rep* 1 9, 1–9 (2019).
134. Nicoll A, Lewis B. Evaluation of the roles of lipoprotein lipase and hepatic lipase in lipoprotein metabolism: in vivo and in vitro studies in man. *Eur J Clin Invest*. 1980;10:487–495.
135. Zannis VI, Breslow JL. Human Very Low Density Lipoprotein Apolipoprotein E Isoform Polymorphism Is Explained by Genetic Variation and Posttranslational Modification. *Biochemistry*. 1981;20:1033–41.
136. Zannis VI, et al. Proposed nomenclature of apoE isoforms, apoE genotypes, and phenotypes. *J Lipid Res*. 1982;23:911–4.
137. Phillips MC. Apolipoprotein E isoforms and lipoprotein metabolism. *IUBMB Life*. 2014;66:616–23.
138. Blum CB, et al. High Density Lipoprotein Metabolism in Man. *J Clin Invest*. 1977;60:795–807.
139. Shepherd J, Packard CJ, Patsch JR, Gotto AM, Taunton JD. Effects of Dietary Polyunsaturated and Saturated Fat on the Properties of High Density Lipoproteins and the Metabolism of Apolipoprotein A-I. *J Clin Invest*. 1978;6:1582–92.
140. Lamarche B, Couture P. Dietary fatty acids, dietary patterns, and lipoprotein metabolism. *Curr Opin Lipidol*. 2015;26:42–7.
141. Lichtenstein AH, et al. 2021 Dietary Guidance to Improve Cardiovascular Health: A Scientific Statement from the American Heart Association. *Circulation*. 2021;144:472–87.
142. Okie S. New York to Trans Fats: You're Out! *N Engl J Med*. 2007;356:2017–21.
143. Goldstein JL, Brown MS. Binding and Degradation of Low Density Lipoproteins by Cultured Human Fibroblasts: comparison of cells from a normal subject and from a patient with homozygous familial hypercholesterolemia. *J Biol Chem*. 1974;249:5153–62.
144. Brown MS, Goldstein JL. Familial hypercholesterolemia: Defective binding of lipoproteins to cultured fibroblasts associated with impaired regulation of 3 hydroxy 3 methylglutaryl coenzyme A reductase activity. *Proc Natl Acad Sci*. 1974;71:788–92.
145. Brundert M, et al. Scavenger receptor class B type I mediates the selective uptake of high-density lipoprotein-associated cholesteryl ester by the liver in mice. *Arterioscler Thromb Vasc Biol*. 2005;25:143–8.
146. Zanoni P, et al. Rare variant in scavenger receptor BI raises HDL cholesterol and increases risk of coronary heart disease. *Science*. 2016;1979(351):1166–71.
147. Van Eck M, et al. Scavenger receptor BI facilitates the metabolism of VLDL lipoproteins in vivo. *J Lipid Res*. 2008;49:136–46.
148. Khera AV, et al. Cholesterol Efflux Capacity, High-Density Lipoprotein Function, and Atherosclerosis. *N Engl J Med*. 2011;364:127–35.
149. Li XM, et al. Paradoxical association of enhanced cholesterol efflux with increased incident cardiovascular risks. *Arterioscler Thromb Vasc Biol*. 2013;33:1696–705.
150. Low H, Hoang A, Sviridov D. Cholesterol efflux assay. *J Visualized Exp*. 2012;61:3791–3810.
151. Jian B, et al. Scavenger receptor class B type I as a mediator of cellular cholesterol efflux to lipoproteins and phospholipid acceptors. *J Biol Chem*. 1998;273:5599–606.
152. Ishibashi S, et al. Hypercholesterolemia in Low Density Lipoprotein Receptor Knockout Mice and its Reversal by Adenovirus-mediated Gene Delivery. *J Clin Invest*. 1993;92:883–93.
153. Huszar D, et al. Increased LDL Cholesterol and Atherosclerosis in LDL Receptor-Deficient Mice With Attenuated Expression of Scavenger Receptor B1. *Arterioscler Thromb Vasc Biol*. 2000;20:1068–73.
154. Yang XP, et al. Scavenger receptor-BI is a receptor for lipoprotein(a). *J Lipid Res*. 2013;54:2450–7.
155. Cal R, et al. Low-density lipoprotein receptor-related protein 1 mediates hypoxia-induced very low density lipoprotein-cholesteryl ester uptake and accumulation in cardiomyocytes. *Cardiovasc Res*. 2012;94:469–79.
156. Niu YG, Evans RD. Myocardial metabolism of triacylglycerol-rich lipoproteins in type 2 diabetes. *J Physiol*. 2009;587:3301–15.
157. Francis GA, Knopp RH, Oram JF. Defective removal of cellular cholesterol and phospholipids by apolipoprotein A-I in Tangier Disease. *J Clin Invest*. 1995;96:78–87.
158. Potere N, et al. Developing LRP1 Agonists into a Therapeutic Strategy in Acute Myocardial Infarction. *Int J Mol Sci*. 2019;20:1–18.
159. Proctor SD, Pabla CK, Mamo JCL. Arterial intimal retention of pro-atherogenic lipoproteins in insulin deficient rabbits and rats. *Atherosclerosis*. 2000;149:315–22.
160. Redgrave TG, Snibson DA. Clearance of chylomicron triacylglycerol and cholesteryl ester from the plasma of streptozotocin-induced diabetic and hypercholesterolemic hypothyroid rats. *Metabolism*. 1977;26:493–503.
161. Niu YG, Evans RD. Metabolism of very-low-density lipoprotein and chylomicrons by streptozotocin-induced diabetic rat heart: Effects of diabetes and lipoprotein preference. *Am J Physiol Endocrinol Metab*. 2008;295:1106–16.
162. Unger RH, Orci L (2002) Lipoapoptosis: its mechanism and its diseases. *Biochimica et Biophysica Acta (BBA)-Molecular and Cell Biology of Lipids*. 1585(2-3):202-12.
163. Zlobine I, Gopal K, Ussher JR (2016) Lipotoxicity in obesity and diabetes-related cardiac dysfunction. *Biochimica et Biophysica Acta (BBA)-Molecular and Cell Biology of Lipids*. 1861(10):1555-68.
164. Van De Weijer T, Schrauwen-Hinderling VB, Schrauwen P. Lipotoxicity in type 2 diabetic cardiomyopathy. *Cardiovasc Res*. 2011;92:10–8.
165. Koseki M, et al. Current Diagnosis and Management of Tangier Disease. *J Atheroscler Thromb*. 2021;28:802–10.
166. Hooper AJ, Hegele RA, Burnett JR. Tangier disease: update for 2020. *Curr Opin Lipidol*. 2020;31:80–4.
167. Brousseau ME, et al. Cellular cholesterol efflux in heterozygotes for Tangier disease is markedly reduced and correlates with high density lipoprotein cholesterol concentration and particle size. *J Lipid Res*. 2000;41:1125–35.
168. Schuler-Luttman S, et al. Cholesterol efflux from normal and Tangier disease fibroblasts into normal, high-density lipoprotein-deficient, and apolipoprotein E-deficient plasmas. *Metabolism*. 2000;49:770–7.
169. Rogler G, Trümbach B, Klima B, Lackner KJ, Schmitz G. HDL-Mediated Efflux of Intracellular Cholesterol Is Impaired in Fibroblasts From Tangier Disease Patients. *Arterioscler Thromb Vasc Biol*. 1995;15:683–90.
170. Hobbs HH, Rader DJ. ABC1: connecting yellow tonsils, neuropathy, and very low HDL. *J Clin Invest*. 1999;104:1015–7.
171. Shaish A, Keren G, Chouraqui P, Levkovitz H, Harats D. Imaging of Aortic Atherosclerotic Lesions by 125I-LDL, 125I-Oxidized-LDL, 125I-HDL and 125I-BSA. *Pathobiology*. 2002;69:225–9.
172. Bozóky Z, et al. Preparation and investigation of 99m technetium-labeled low-density lipoproteins in rabbits with experimentally induced hypercholesterolemia. *Eur Biophys J*. 2004;33:140–5.
173. Yong-Sang J, et al. Development, synthesis, and 68Ga-Labeling of a Lipophilic complexing agent for atherosclerosis PET imaging. *Eur J Med Chem*. 2019;176:129–34.

174. Zheng KH, et al. HDL mimetic CER-001 targets atherosclerotic plaques in patients. *Atherosclerosis*. 2016;251:381–8.
175. Toner YC, Prévot G, van Leent MM, Munitz J, Oosterwijk R, Verschuur AV, et al. Macrophage PET imaging in mouse models of cardiovascular disease and cancer with an apolipoprotein-inspired radiotracer. *npj Imaging*. 2024;2(1):12.
176. Allison E, Edirimanne S, Matthews J, Fuller SJ. Breast Cancer Survival Outcomes and Tumor-Associated Macrophage Markers: A Systematic Review and Meta-Analysis. *Oncol Ther*. 2023;11:27–48.
177. Sambandam N, et al. Metabolism of VLDL is increased in streptozotocin-induced diabetic rat hearts. *Am J Physiol Heart Circ Physiol*. 2000;278:1874–82.
178. Björnheden T, Bondjers G, Wiklund O. Direct Assessment of Lipoprotein Outflow From In Vivo-Labeled Arterial Tissue as Determined in an In Vitro Perfusion System. *Arterioscler Thromb Vasc Biol*. 1998;18:1927–33.
179. Osborne JC, Schaefer EJ, Powell GM, Lee NS, Zech LA. Molecular Properties of Radioiodinated Apolipoprotein A-I. *J Biol Chem*. 1984;259:347–53.
180. Schaefer EJ, et al. Metabolism of high density lipoprotein subfractions and constituents in Tangier disease following the infusion of high density lipoproteins. *J Lipid Res*. 1981;22:217–28.
181. Owens RJ, et al. Apolipoprotein A-I and its amphipathic helix peptide analogues inhibit human immunodeficiency virus-induced syncytium formation. *J Clin Invest*. 1990;86:1142–50.
182. Remaley AT, et al. Synthetic amphipathic helical peptides promote lipid efflux from cells by an ABCA1-dependent and an ABCA1-independent pathway. *J Lipid Res*. 2003;44:828–36.
183. Tran-Dinh A, et al. HDL and endothelial protection. *Br J Pharmacol*. 2013;169:493.
184. Calabresi L, Gomaschi M, Franceschini G. Endothelial Protection by High-Density Lipoproteins. *Arterioscler Thromb Vasc Biol*. 2003;23:1724–31.
185. Soran H, Schofield JD, Durrington PN. Antioxidant properties of HDL. *Front Pharmacol*. 2015;6:1–6.
186. Assmann G, Gotto AM. HDL Cholesterol and Protective Factors in Atherosclerosis. *Circulation*. 2004;109:1–7.
187. Rader DJ, Hovingh GK. HDL and cardiovascular disease. *The Lancet*. 2014;384:618–25.
188. Kingwell BA, Chapman MJ. Future of high-density lipoprotein infusion therapies: Potential for clinical management of vascular disease. *Circulation*. 2013;128:1112–21.
189. Shaw JA, et al. Infusion of Reconstituted High-Density Lipoprotein Leads to Acute Changes in Human Atherosclerotic Plaque. *Circ Res*. 2008;103:1084–91.
190. Begue F, Apalama ML, Lambert G, Meilhac O. HDL as a Treatment Target: Should We Abandon This Idea? *Curr Atheroscler Rep*. 2023;25:1093–9.
191. Karalis I, Jukema JW. HDL Mimetics Infusion and Regression of Atherosclerosis: Is It Still Considered a Valid Therapeutic Option? *Curr Cardiol Rep*. 2018;20:1–8.
192. Zheng KH, et al. No benefit of HDL mimetic CER-001 on carotid atherosclerosis in patients with genetically determined very low HDL levels. *Atherosclerosis*. 2020;311:13–9.
193. Chehab O, et al. Higher HDL cholesterol levels are associated with increased markers of interstitial myocardial fibrosis in the MultiEthnic Study of Atherosclerosis (MESA). *Sci Rep*. 2023;13:1–9.
194. Casula M, Colpani O, Xie S, Catapano AL, Baragetti A. HDL in Atherosclerotic Cardiovascular Disease. In Search of a Role Cells. 2021;10:1–17.
195. Hofstraat SRJ, et al. Nature-inspired platform nanotechnology for RNA delivery to myeloid cells and their bone marrow progenitors. *Nat Nanotechnol*. 2025;2025:1–11.
196. Hernández-Jiménez T, et al. 225Ac-rHDL Nanoparticles: A Potential Agent for Targeted Alpha-Particle Therapy of Tumors Overexpressing SR-BI Proteins. *Molecules*. 2022;27:1–15.
197. Braza MS, et al. Inhibiting Inflammation with Myeloid Cell-Specific Nanobiologics Promotes Organ Transplant Acceptance. *Immunity*. 2018;49:819–28.
198. Binderup T, et al. Imaging-assisted nanoimmunotherapy for atherosclerosis in multiple species. *Sci Transl Med*. 2019;11:1–13.
199. McMahon KM, et al. Biomimetic high density lipoprotein nanoparticles for nucleic acid delivery. *Nano Lett*. 2011;11:1208–14.
200. Wolfrum C, et al. Mechanisms and optimization of in vivo delivery of lipophilic siRNAs. *Nat Biotechnol*. 2007;25:1149–57.
201. Nakayama T, et al. Harnessing a physiologic mechanism for siRNA delivery with mimetic lipoprotein particles. *Mol Ther*. 2012;20:1582–9.
202. Pérez-Medina C, Teunissen AJP, Kluza E, Mulder WJM, van der Meel R. Nuclear imaging approaches facilitating nanomedicine translation. *Adv Drug Deliv Rev*. 2020;154:123–41.
203. Schrijver DP et al. Nanoengineering apolipoprotein A1-based immunotherapeutics. *Adv Therap*. 2021;4:1–6.
204. Van Leent MMT, et al. Prosaposin mediates inflammation in atherosclerosis. *Sci Transl Med*. 2021;13:1–13.
205. Aluicio-Sarduy E, Barnhart TE, Weichert J, Hernandez R, Engle JW. Cyclotron-Produced <sup>132</sup>La as a PET Imaging Surrogate for Therapeutic <sup>225</sup>Ac. *J Nucl Med*. 2021;62:1012–5.
206. Pratt EC, et al. Simultaneous quantitative imaging of two PET radiotracers via the detection of positron–electron annihilation and prompt gamma emissions. *Nat Biomed Eng*. 2023;7:1–12.
207. Cherry SR, et al. Total-Body PET: Maximizing Sensitivity to Create New Opportunities for Clinical Research and Patient Care. *J Nucl Med*. 2018;59:3–12.
208. Katal S, Eibschutz LS, Saboury B, Gholamrezanezhad A, Alavi A. Advantages and Applications of Total-Body PET Scanning. *Diagnostics*. 2022;12:1–13.
209. Tardif J-C, et al. Effects of reconstituted high-density lipoprotein infusions on coronary atherosclerosis: a randomized controlled trial. *JAMA*. 2007;297:1675–82.
210. Tardif J-C, et al. Effects of the high-density lipoprotein mimetic agent CER-001 on coronary atherosclerosis in patients with acute coronary syndromes: a randomized trial. *Eur Heart J*. 2014;35:3277–86.
211. Degoma EM, Rader DJ. Novel HDL-directed pharmacotherapeutic strategies. *Nat Rev Cardiol*. 2011;8:266–77.
212. De Jesus M, Wurm FM. Manufacturing recombinant proteins in kg-ton quantities using animal cells in bioreactors. *Eur J Pharm Biopharm*. 2011;78:184–8.
213. Morla-Folch J, Ranzenigo A, Fayad ZA, Teunissen AJP. Nanotherapeutic Heterogeneity: Sources, Effects, and Solutions. *Small*. 2024;20:2307502.
214. Han JY, La Fiandra JN, DeVoe DL. Microfluidic vortex focusing for high throughput synthesis of size-tunable liposomes. *Nat, Comm*. 2022;13:6997–7008.
215. Darabi M, Guillas-Baudouin I, Le Goff W, Chapman MJ, Kon-tush A. Therapeutic applications of reconstituted HDL: When structure meets function. *Pharmacol Ther*. 2016;157:28–42.
216. Kim JS, Kang Y, Son KH, Choi SM, Kim KY. Manufacturing and shelf stability of reconstituted high-density lipoprotein for infusion therapy. *Biotechnol Bioprocess Eng*. 2011;16:785–92.
217. Pownall HJ, Rosales C, Gillard BK, Ferrari M. Native and Reconstituted Plasma Lipoproteins in Nanomedicine: Physicochemical Determinants of Nanoparticle Structure, Stability, and Metabolism. *Methodist Debakey Cardiovasc J*. 2016;12:146–51.
218. Schwendeman A, et al. The effect of phospholipid composition of reconstituted HDL on its cholesterol efflux and anti-inflammatory properties. *J Lipid Res*. 2015;56:1727.

219. Chen W, et al. RGD peptide functionalized and reconstituted high-density lipoprotein nanoparticles as a versatile and multimodal tumor targeting molecular imaging probe. *FASEB J.* 2010;24:1689–99.
220. Liu L, et al. Hyaluronic acid-decorated reconstituted high density lipoprotein targeting atherosclerotic lesions. *Biomaterials.* 2014;35:8002–14.
221. Zhu C, Xia Y. Biomimetics: reconstitution of low-density lipoprotein for targeted drug delivery and related theranostic applications. *Chem Soc Rev.* 2017;46:7668–82.
222. Andraski AB, Sacks FM, Aikawa M, Singh SA. Understanding HDL Metabolism and Biology Through in Vivo Tracer Kinetics. *Arterioscler Thromb Vasc Biol.* 2024;44:76–88.

**Publisher's Note** Springer Nature remains neutral with regard to jurisdictional claims in published maps and institutional affiliations.

Springer Nature or its licensor (e.g. a society or other partner) holds exclusive rights to this article under a publishing agreement with the author(s) or other rightsholder(s); author self-archiving of the accepted manuscript version of this article is solely governed by the terms of such publishing agreement and applicable law.